Acta Geologica Polonica, Vol. 73 (2023), No. 1, pp. 33–62
DOI: 10.24425/agp.2022.140431

Integrated biostratigraphy and palaeoenvironments of the Upper Cretaceous in the Petrich section (Central Srednogorie Zone, Bulgaria)

POLINA PAVLISHINA[1]*, DOCHO DOCHEV[1], MICHAEL WAGREICH[2] and VERONIKA KOUKAL[2]

[1] *Department of Geology, Paleontology and Fossil Fuels, Faculty of Geology and Geography, Sofia University "St. Kliment Ohridski", Sofia, Bulgaria; e-mails: polina@gea.uni-sofia.bg; dochev@gea.uni-sofia.bg*
[2] *Department of Geology, University of Vienna, A-1090 Vienna, Austria; e-mails: michael.wagreich@univie.ac.at; veronika.koukal@univie.ac.at*
** Corresponding author*

ABSTRACT:

Pavlishina, P., Dochev, D., Wagreich, M. and Koukal, V. 2023. Integrated biostratigraphy and palaeoenvironments of the Upper Cretaceous in the Petrich section (Central Srednogorie Zone, Bulgaria). *Acta Geologica Polonica*, **73** (1), 33–62. Warszawa.

The Upper Cretaceous succession (Coniacian to lowermost Maastrichtian, with focus on the Campanian) at Petrich, Central Srednogorie Zone in Bulgaria, is described and calibrated stratigraphically based on nannofossils, dinoflagellate cysts and inoceramids. The following standard nannofossil zones and subzones are identified: UC10–UC11ab (middle to upper Coniacian), UC11c–UC12–UC13 (uppermost Coniacian to Santonian), UC14a (lowermost Campanian), UC14b^{TP}–UC15c^{TP} (lower Campanian to 'middle' Campanian), UC15d^{TP}–UC15e^{TP} (upper Campanian), UC16a^{TP} (of Thibault *et al*. 2016; upper part of the upper Campanian), and UC16b (Campanian–Maastrichtian boundary). The base of the Campanian is defined by the FO of *Broinsonia parca parca* (Stradner) Bukry, 1969 and *Calculites obscurus* (Deflandre) Prins and Sissingh in Sissingh, 1977 (a morphotype with a wide central longitudinal suture). The *Areoligera coronata* dinoflagellate cyst Zone (upper lower Campanian to upper upper Campanian) is identified, corresponding to the UC14b^{TP}–UC16a^{TP} nannofossil subzones. The inoceramid assemblage indicates the '*Inoceramus*' *azerbaydjanensis*–'*Inoceramus*' *vorhelmensis* Zone, correlated within the interval of nannofossil subzones UC15d^{TP}–UC15e^{TP}. The composition of the dinoflagellate cyst assemblages and palynofacies pattern suggest normal marine, oxic conditions and low nutrient availability within a distal shelf to open marine depositional environment during the Campanian.

Key words: Upper Cretaceous; Campanian; Calcareous nannofossils; Dinoflagellate cysts; Inoceramids; Biostratigraphy; Palaeoenvironments.

INTRODUCTION

The upper part of the Upper Cretaceous (the 'Senonian' in older terms; d'Orbigny 1842) comprises the Coniacian, Santonian, Campanian and Maastrichtian (89.39–66.04 Ma; Gale *et al*. 2020) and archives a major change in the Earth system and palaeoclimate, from the mid-Cretaceous hothouse to cooler greenhouse conditions (e.g., Hay and Floegel 2012). Especially the Campanian (83.65–72.17 Ma; Gale *et al*. 2020), the longest stage of the Upper Cretaceous, represents a major turning point in Earth history, considering palaeoclimate and palaeoceanography. The Campanian is characterized by a generally high sea level and decreasing global surface temperatures after the Cretaceous Thermal Maximum

around the Cenomanian–Turonian (Haq *et al*. 1987; Jenkyns *et al*. 1994; Hardenbol *et al*. 1998; Clarke and Jenkyns 1999; Huber *et al*. 2002; Hay and Flögel 2012). Increasing marine seaways and oceanic turnover has led to a transition from typical Mesozoic to 'modern' oceanic circulation, including the final oceanic anoxic event OAE 3 in the Santonian (Premoli Silva and Sliter 1999; Wagreich 2012; Mansour and Wagreich 2022). The detailed understanding of such Late Cretaceous environmental changes requires a precise stratigraphical framework, including the characterization of important bloom groups such as inoceramids, calcareous nannofossils and dinoflagellate cysts (dinocysts).

The biostratigraphy of the 'Senonian', and especially of the Campanian, is already well-established, based on different important fossil groups, such as ammonites in US Western Interior Basin (see Cobban *et al*. 2006), inoceramids (Walaszczyk 1992, 1997, 2004; Walaszczyk *et al*. 2001, 2008), and calcareous nannofossils (e.g., UC zonation by Burnett 1998) (see the review in Gale *et al.* 2020). Their zones and ranges have provided a firm dataset for the subdivision of the Campanian and detailed correlation. Dinoflagellate cysts seem to be a group with a rising potential for the stratigraphic subdivision of the Late Cretaceous and especially the Campanian and its boundaries, supported by studies from both the Tethyan and Boreal realm (Kirsch 1991; Roncaglia and Corradini 1997; Antonescu *et al*. 2001; Schiøler and Wilson 2001; Roncaglia 2002; Skupien and Mohamed 2008; Radmacher *et al*. 2014; Slimani *et al*. 2021; Niechwedowicz and Walaszczyk 2022). These studies provide valuable information on dinoflagellate cyst ranges, as well as first and last occurrence events (FO and LO) for establishing a sound palynostratigraphic framework of the Campanian. Dinoflagellate cysts assemblages can also infer information to interpret the depositional environments in terms of water depth, depositional energy, temperature, nutrient availability and productivity by using the ratio of peridinioid to gonyaulacoid (P/G) dinocysts and palaeoenvironmental sensitive dinocyst groups (Brinkhuis 1994; Wilpshaar and Leereveld 1994; Zonneveld *et al*. 2013; Frieling and Sluijs 2018; Houben *et al*. 2019; Niechwedowicz *et al*. 2021).

The present paper reports first results of an integrated stratigraphic investigation of the Petrich section, Central Srednogorie Zone in Bulgaria, with special emphasis on the Campanian. Our study creates a comprehensive calibrated dataset for the Campanian, in which dinoflagellate cyst and nannofossil taxa ranges and inoceramid occurrences provide valuable markers for the age assessment and the stratigraphic subdivision of the Campanian. Palaeoenvironmental analysis in this study is mainly based on dinocyst assemblages and palynofacies data.

GEOLOGICAL SETTING

The Srednogorie Zone in Bulgaria represents a chain of strike-slip and pull-apart basins, which are a part of the peri-Tethyan arc/back-arc basin system (Ivanov 2017; Vangelov *et al*. 2019). The Upper Cretaceous volcano-sedimentary sequence in the western part of the Central Srednogorie tectonic subzone forms two strips called the Chelopech and Panagyurishte strips, spanning the Turonian–Maastrichtian and unconformably overlying different pre-Cretaceous rocks (Text-fig. 1). In the Srednogorie Zone, the Upper Cretaceous is represented by various rock successions, including siliciclastic sequences, volcanoclastic and epiclastic deposits, which are overlain by white, red and grey limestones, with a fast transition into sandy, low-density turbidites. The similarities between these strips (in lithological and chronostratigraphical terms) allow to assume the presence of either a single Cretaceous basin or a connected basin system, disrupted by Cenozoic tectonics.

According to Vangelov *et al.* (2019), the Upper Cretaceous volcano-sedimentary sequence in the entire Panagyurishte strip comprises a basal siliciclastic terrigenous unit (middle Turonian), a volcanoclastic unit (upper Turonian), an overlying lower epiclastic unit (Coniacian–lower Santonian), the pelagic Mirkovo Formation (Santonian–lower Campanian), an upper epiclastic unit (upper Campanian) and the Chugovitsa Formation (upper Campanian–Maastrichtian) (see Text-figs 1, 2).

One of the most representative and continuous sedimentary sequences in the Panagyurishte strip is exposed in the vicinity of Petrich village (Text-figs 2, 3). The herein newly studied Petrich section, with a total thickness of 596 m, is cropping out 1 km east of the village of Petrich and is here described in detail. In the Petrich section, the lithostratigraphical units mentioned above are with a confined chronostratigraphic range as follows: the base of the section is composed of limy, medium-bedded, mica-bearing volcanoclastic sandstones assigned to the so-called lower epiclastic unit (lower Coniacian), followed by thin- to medium-bedded grey, pink and red, sometimes mottled limestones of the Mirkovo Formation (Moev and Antonov 1978; CORB sensu Wang *et al*. 2011) (middle Coniacian–lower Campanian;

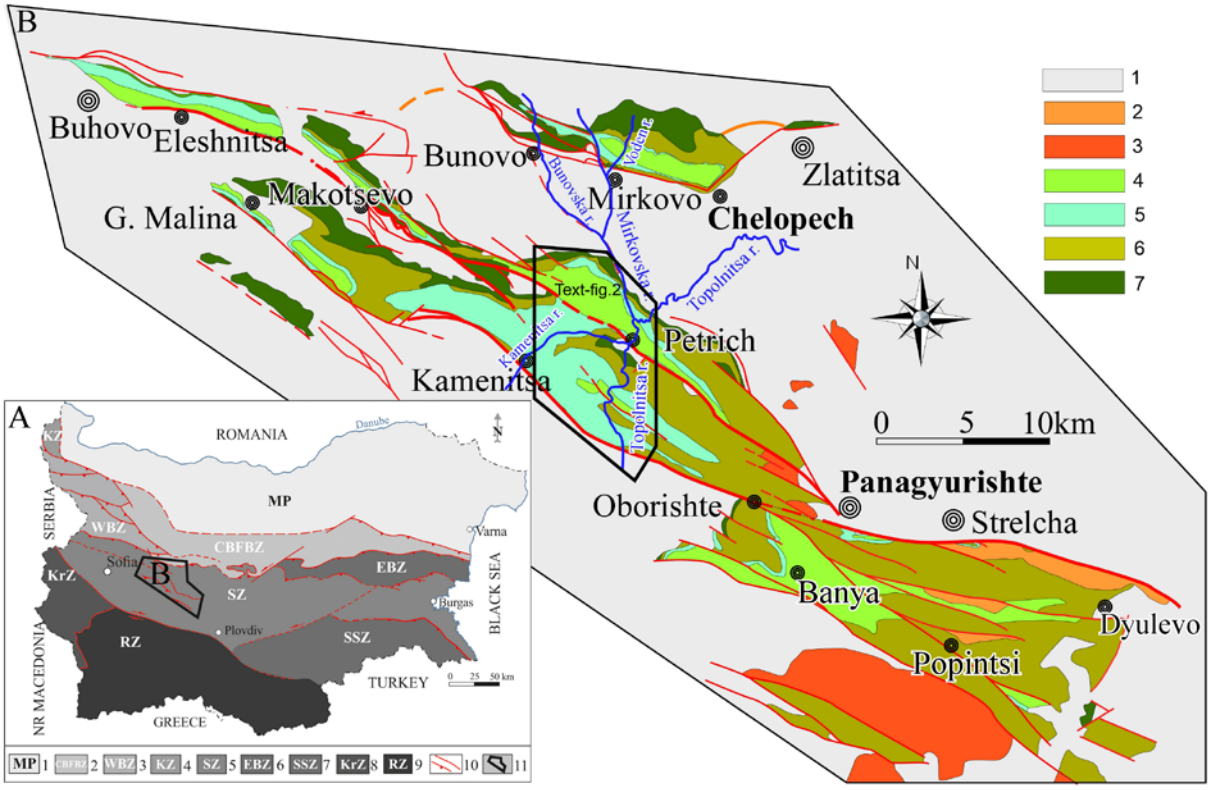

Text-fig. 1. Location of the study area. **A** – Tectonic sketch map of Bulgaria showing the position of the Chelopech and Panagyurishte strips (after Ivanov 2017): 1 – Moesian Platform, 2 – Central Balkan–Fore-Balkan Zone, 3 – West Balkan Zone, 4 – Kula Zone, 5 – Srednogorie Zone, 6 – East Balkan Zone, 7 – Sakar-Strandhza Zone, 8 – Kraisthe Zone, 9 – Rhodope Zone, 10 – Main faults and thrusts, 11 – outline of the study area. **B** – Geological sketch map of the Upper Cretaceous volcano-sedimentary sequences exposed in the Chelopech and Panagyurishte strips (after Vangelov *et al.* 2019): 1 – pre-Cretaceous basement, 2 – Paleocene, 3 – Upper Cretaceous plutons, 4 – Chugovitsa Formation, 5 – Mirkovo Formation, 6 – volcano-terrigenous complex, 7 – basal terrigenous unit.

Text-fig. 3). The middle and upper parts of the section consist of muddy turbidites of the Chugovitsa Formation (Campanian–Maastrichtian), composed of an alternation of thin to medium-bedded silty marlstones, marlstones and sandstones. The lower part of the Chugovitsa Formation, known as the Voden Member (Moev and Antonov 1978) is 83 m thick and comprises grey thin-bedded marlstones, intercalated with rare sandstone beds. The Voden Member of the Chugovitsa Formation yielded comparatively rich macro- and microfossil assemblages (Text-fig. 3). This complete and uninterrupted part of the Petrich section has been studied.

MATERIAL AND METHODS

The Petrich section was sampled for dinoflagellate cysts and calcareous nannofossils during two field campaigns in order to document its biostratigraphy. Thirty-five palyno- and nannofossil, cross-calibrated samples were collected during the first field campaign in 2020. Additional sampling took place in August 2021 in the framework of the joint Bulgarian-Austrian project (WTZ, KP-06-Austria/9) and a total of forty-five samples were investigated. Inoceramids were collected during both field campaigns, but found only in one level – in the upper part of bed 21 (Voden Member of the Chugovitsa Formation) (Text-fig. 3).

Palynological samples were processed at the Polish Academy of Sciences, Laboratory of the Geological Sciences Institute, Kraków (Poland). About 50 g of sediment was processed by HCl and HF treatment and heavy liquid separation. The residues were finally sieved through 10 µm nylon meshes. Strew mounts were made in glycerine jelly. From each sample, two palynological strew mounts were prepared and analyzed for their palynological content. The slides are stored in the collections of the Sofia University "St. Kliment Ohridski", Bulgaria.

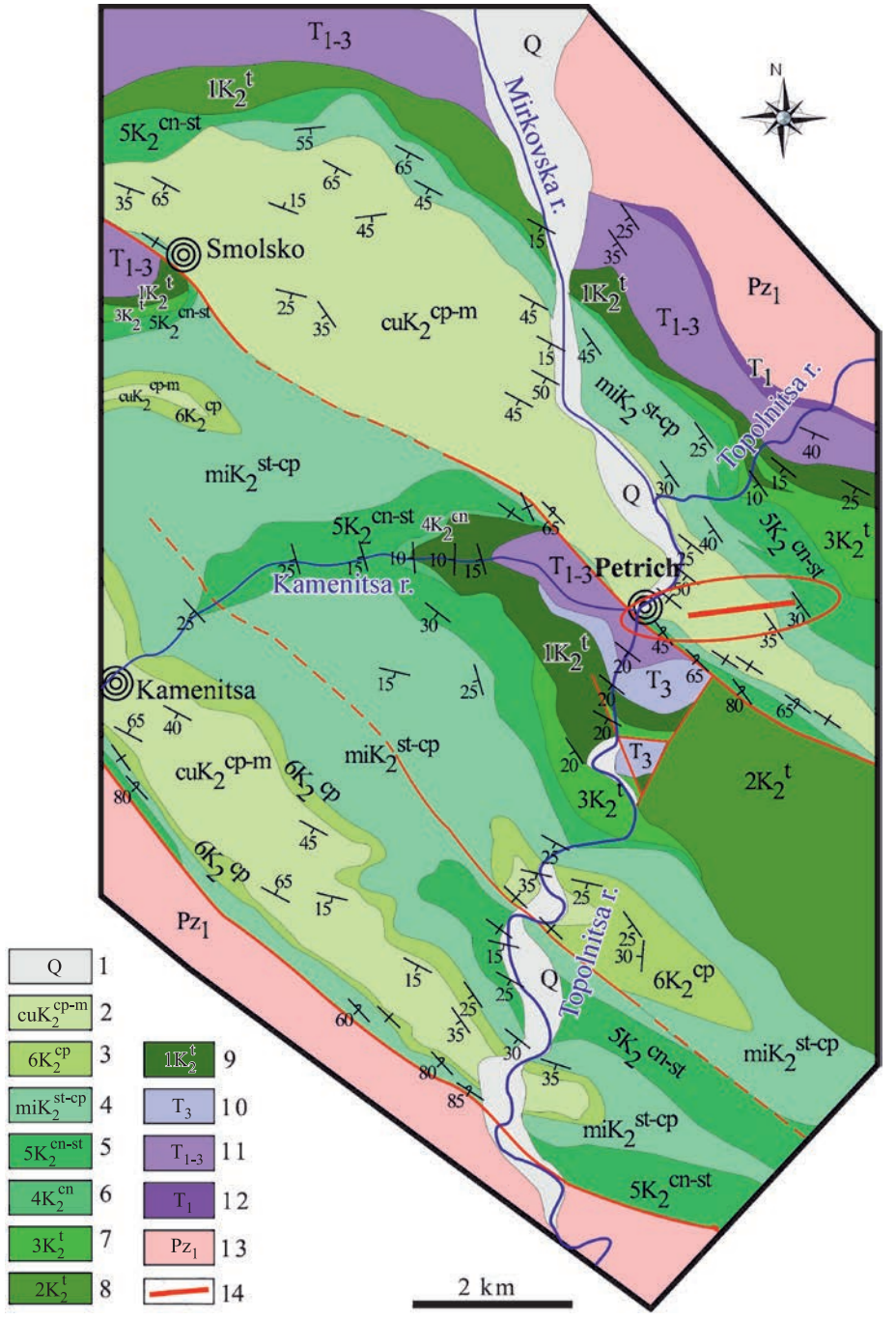

Text-fig. 2. Geological sketch map of the area of the Petrich village (after Vangelov *et al.* 2019). 1 – Quaternary (Q), 2 – Chugovitsa Formation (cuK_2^{cp-mt}), 3 – upper epiclastic unit ($6K_2^{cp}$), 4 – Mirkovo Formation (miK_2^{st-cp}), 5 – lower epiclastic unit ($5K_2^{cn-st}$), 6 – marl-limestone unit ($4K_2^{cn}$), 7 – volcanoclastic unit ($3K_2^{t}$), 8 – Vran Kamak magmatic centre ($2K_2^{t}$), 9 – basal terrigenous unit ($1K_2^{t}$), 10 – Moesian Terrigenous-Carbonate Group (T^3), 11 – Iskar Carbonate Group ($T_{1–3}$), 12 – Petrohan Terrigenous Group (T_1), 13 – Palaeozoic high-grade metamorphites (Pz_1), 14 – location of the section studied.

Text-fig. 3. Lithological column of the Petrich section (Bulgaria) with ranges of selected dinoflagellate cysts (black), calcareous nannofossils (red) and inoceramid taxa (blue). 1 – limy, medium-bedded volcanoclastic sandstones with muscovite, 2 – thin-bedded limy siltstones, 3 – grey, medium-bedded silty limestones, 4 – grey, medium-bedded limestones, 5 – grey, thin-bedded limestones, 6 – red to pink medium-bedded limestones, 7 – thin-bedded red to pink limestones, 8 – yellow to yellowish limestones, 9 – unclearly bedded limestones, 10 – not well exposed limestones, 11 – red marlstones, 12 – grey marlstones, 13 – thin- to medium-bedded sandstones, 14 – inoceramid bivalves, 15 – samples for dinoflagellate cysts, 16 – samples for calcareous nannofossils, 17 – '*Inoceramus*' *azerbaydjanensis* – '*Inoceramus*' *vorhelmensis* Zone. →

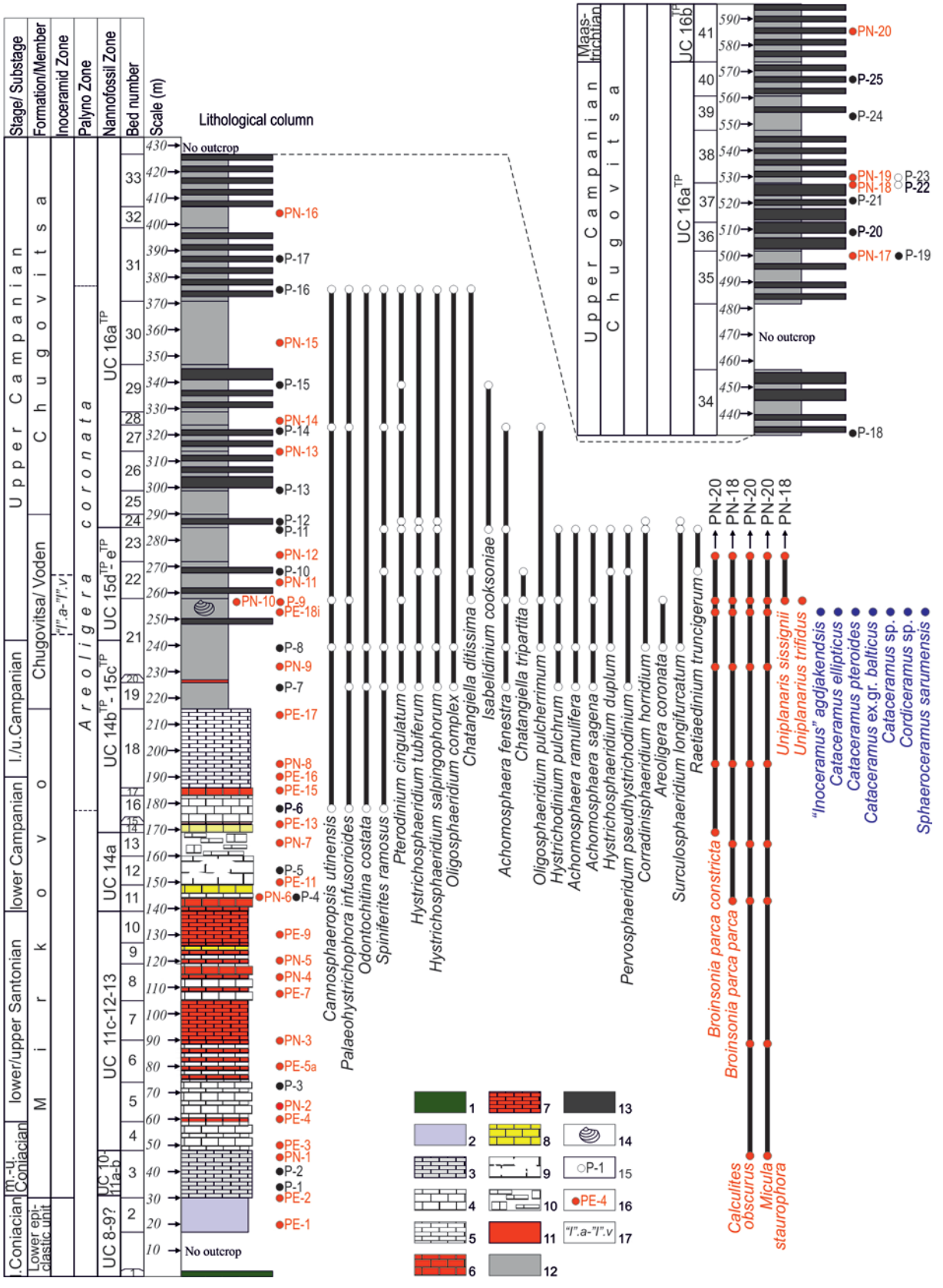
Stage/ Substage
Formation/Member
Inoceramid Zone
Palyno Zone
Nannofossil Zone
Bed number
Scale (m)
Lithological column
Upper Campanian
Chugovitsa
Mirkovo
Areoligera coronata
m.-u. Coniacian
lower/upper Santonian
l./u.Campanian
lower Campanian
Chugovitsa/ Voden
Lower epi-clastic unit
UC 8-9?
UC 10-11a-b
UC 11c-12-13
UC 14a
UC 14b^TP - 15c^TP
UC 15d^TP - e^TP
UC 16a^TP
UC 16b^TP
Maas-trichtian
No outcrop
Cannosphaeropsis utinensis
Palaeohystrichophora infusorioides
Odontochitina costata
Spiniferites ramosus
Pterodinium cingulatum
Hystrichosphaeridium tubiferum
Hystrichosphaeridium salpingophorum
Oligosphaeridium complex
Chatangiella ditissima
Isabelidinium cooksoniae
Achomosphaera fenestra
Chatangiella tripartita
Oligosphaeridium pulcherrimum
Hystrichodinium pulchrum
Achomosphaera ramulifera
Achomosphaera sagena
Hystrichosphaeridium duplum
Pervosphaeridium pseudhystrichodinium
Corradinisphaeridium horridium
Areoligera coronata
Surculosphaeridium longifurcatum
Raetiaedinium truncigerum
Broinsonia parca constricta
Broinsonia parca parca
Calculites obscurus
Micula staurophora
Uniplanaris sissignii
Uniplanarius trifidus
"Inoceramus" agdjakendsis
Cataceramus ellipticus
Cataceramus pteroides
Cataceramus ex.gr. balticus
Cataceramus sp.
Cordiceramus sp.
Sphaeroceramus sarumensis
PN-20
PN-18
PN-20
PN-20
PN-18
P-25
P-24
PN-19
PN-18
P-23
P-22
P-21
P-20
PN-17
P-19
P-18

The readers are referred to Fensome *et al.* (2019) for dinoflagellate cyst taxonomy.

Quantitative analysis of dinocyst associations were based on counts of 100 specimens, where possible, per slide. These are described in terms of rare (1–9 specimens), common (10–20 specimens) and abundant (more than 20 specimens). Palynofacies analysis involved counting the relative abundance of sedimentary organic constituents based on 400 particles per slide. Three main groups of kerogen constituents proposed by Tyson (1995), Radmacher *et al.* (2020) and Slimani *et al.* (2021) have been recognized in the slides, namely: 1) phytoclasts (opaque and translucent organic particles), 2) palynomorphs (dinoflagellate cysts, spores and pollen), and 3) amorphous organic matter (AOM). The data were plotted in the ternary AOM–Phytoclast–Palynomorph plot of Tyson (1993) and in the Microplankton–Spore–Pollen ternary plot (after Fedorova 1977; Duringer and Doubinger 1985). Palynofacies parameters, such as the ratio of continental to marine particles (C/M ratio), the ratio of opaque to translucent phytoclasts (OP/TR ratio) (Tyson 1993, 1995), as well as the ratio of peridinioid to gonyaulacoid (P/G) dinocysts (Brinkhuis 1994; Wilpshaar and Leereveld 1994; Harris and Tocher 1997; Schiøler *et al.* 1997; Sluijs *et al*. 2005; Zonneveld *et al*. 2013; Frieling and Sluijs 2018; Houben *et al*. 2019; Niechwedowicz *et al*. 2021) were estimated to characterize the palaeoenvironmental settings.

Nannofossil samples from the studied section were taken at different sampling intervals according to outcrop conditions, vegetation and soil-covered intervals. All in all, forty-five suspension slides were prepared for calcareous nannofossil investigation using scratched sediment powder suspended with distilled water in a beaker (e.g., Wolfgring *et al*. 2018). After two hours, the superfluent was removed, and a new suspension was prepared from which droplets were put on a glass cover plate, air dried and then fixed with Canada Balsam© on a glass slide. The slides were examined qualitatively for nannofossil biostratigraphy using a polarised light microscope (Zeiss Orthoplan, 100× oil immersion objective). In total, thirty-nine samples from the Petrich section yielded a nannofossil record from the interval spanning bed 2 (20 m) through to bed 41 (585 m) (Text-fig. 3). For taxonomy and nannofossil standard zonation, we use Burnett (1998) and NANNOTAX3 (https://www.mikrotax.org/Nannotax3/), except for the Campanian–Maastrichtian boundary interval, where we use emended subzones UC16a^{TP} (uppermost Campanian) and UC16b^{TP} (lowermost Maastrichtian), according to Thibault *et al*. (2016).

Inoceramid bivalves (thirty-nine specimens) were collected from medium-bedded mudstones and most of them are preserved as single valve internal moulds, rarely with shell fragments attached. Due to sediment compaction, most of the specimens are slightly deformed, with some degree of cracking and crushing. In many cases the rugae are displaced with deformed direction. For photography, the inoceramid specimens were covered with ammonium chloride and illustrated in natural size. The specimens used for this work are stored at the inoceramid collection of the Museum of Palaeontology and Historical Geology of the Sofia University "St. Kliment Ohridski", Bulgaria.

CAMPANIAN AND MAASTRICHTIAN STAGE AND SUBSTAGE SUBDIVISION

The Petrich section includes biostratigraphic records of several inferred stage boundaries of the Upper Cretaceous, i.e., Santonian, Campanian and Maastrichtian. However, the presence of the Coniacian–Santonian boundary interval is only inferred from a somehow poorly preserved nannofossil record without correlation to other fossil groups, therefore, we restrain from discussing this boundary in more detail. The reader is referred to the GSSP data published by Lamolda *et al*. (2014), with the first occurrence (FO) of the inoceramid bivalve *Platyceramus undulatoplicatus* (Roemer, 1852) as the boundary marker.

The Campanian Stage was introduced by Coquand (1857). In Europe, its base was originally defined with the lowermost occurrence of the ammonoid species *Placenticeras bidorstaum* (de Grossouvre, 1901) (e.g., Birkelund *et al*. 1984). The last occurrence of the stemless crinoid *Marsupites testudinarius* (Schlotheim, 1820) has been also proposed as a marker for this boundary (Gale *et al.* 1995; Hancock and Gale 1996). Due to the limited occurrence of *Marsupites* spp. in certain palaeoenvironments and palaeogeographic realms, discussion has started to define the base of the Campanian at the lower boundary of the reversed polarity chron C33r (Ogg and Hinnov 2012; Wolfgring *et al*. 2018; Gale *et al*. 2021). In the North American Western Interior Basin, the base of the Campanian is correlated to the base of the *Scaphites leei* III ammonite zone (Cobban *et al*. 2006).

In general, the Campanian stage is subdivided either into two substages, or into a lower, middle and upper substage – but no substage boundary markers or GSSP definitions have been yet proposed (Ogg and Hinnov 2012; Gale *et al*. 2020). In the US Western Interior, the

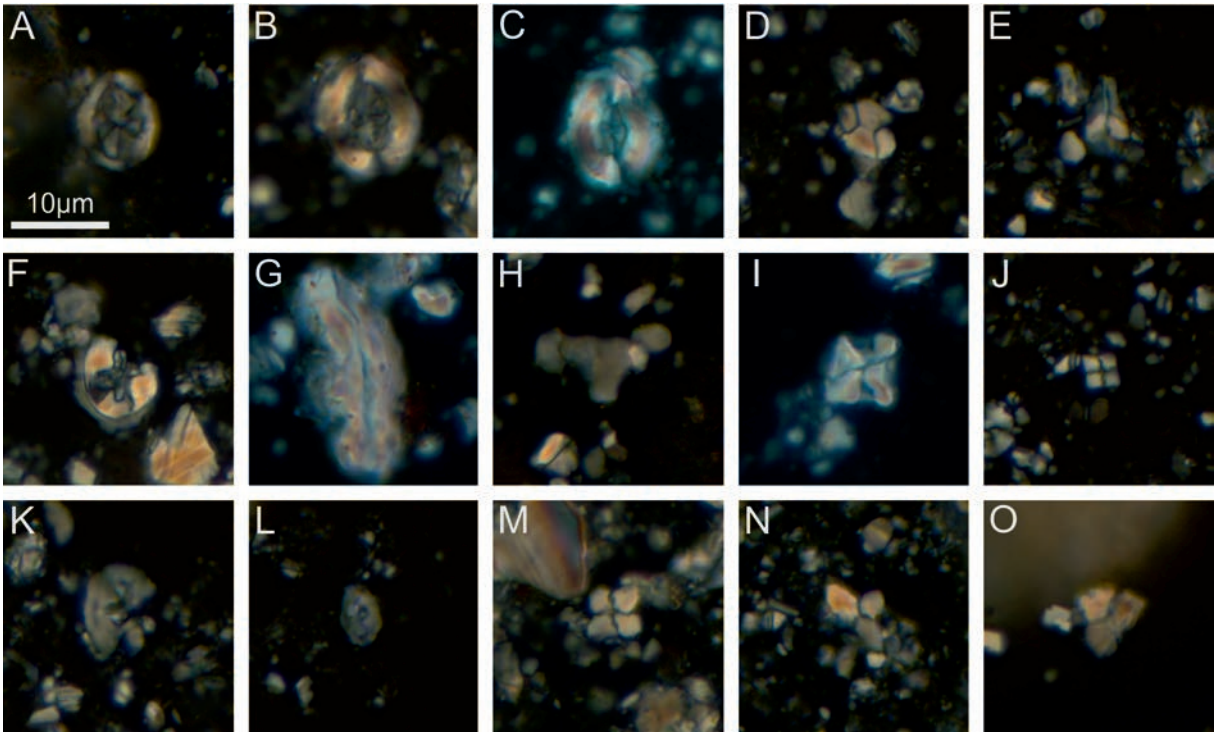

Text-fig. 4. Biostratigraphically significant nannofossil species of the Petrich section, Bulgaria. **A** – *Arkhangelskiella cymbiformis* Vekshina, 1959, sample PE-18b, bed 21. **B** – *Broinsonia parca parca* (Stradner) Bukry, 1969, sample PN-12, bed 23. **C** – *Broinsonia parca constricta* Hattner, Wind and Wise, 1980, sample PN-12, bed 23. **D** – *Calculites obscurus* (Deflandre) Prins and Sissingh in Sissingh, 1977, wide morphotype, sample PN-10, bed 21. **E** – *Ceratolithoides aculeus* (Stradner) Prins and Sissingh in Sissingh, 1977, sample PN-12, bed 23. **F** – *Eiffellithus eximius* (Stover) Perch-Nielsen, 1968, broken specimen, probably reworked, sample PN-20, bed 41. **G** – *Lucianorhabdus cayeuxii* Deflandre, 1959, curved morphotype, sample PE-13, bed 15. **H** – *Marthasterites inconspicuus* Deflandre, 1959, sample PE-7, bed 8. **I** – *Micula staurophora* (Gardet) Stradner, 1963, sample PN-12, bed 23. **J** – *Quadrum* cf. *gartneri* Prins and Perch-Nielsen in Manivit *et al*., 1977, sample PN-12, bed 23. **K** – *Reinhardtites levis* Prins and Sissingh in Sissingh, 1977, broken specimen, sample PN-15, bed 30. **L** – *Tranolithus orionatus* (Reinhardt) Reinhardt, 1966, sample PN-20, bed 41. **M** – *Uniplanarius gothicus* (Deflandre) Hattner and Wise in Wind and Wise, 1983, sample PE-18b, bed 21. **N** – *Uniplanarius sissinghii* (Perch-Nielsen) Farhan, 1987, broken specimen, sample PE-18b, bed 21. **O** – *Uniplanarius trifidus* (Stradner in Stradner and Papp) Hattner and Wise in Wind and Wise, 1983, sample PE-18a, bed 21. All microscope photographs with crossed nicols and same scale (scale bar in A is 10 µm). For position of samples in section see Text-fig. 3.

three-partite subdivision of the Campanian is widely accepted (Cobban *et al.* 2006), whereas in Europe only the lower and upper Campanian are more commonly used, and provisionally reffered to herein. The first occurrence of *Belemnitella mucronata* (Schlotheim, 1813) marked the lower/upper Campanian boundary in northwest Europe (Christensen 1999), which is slightly below the middle/upper Campanian boundary in the North American three-partite subdivision (Ogg and Hinnov 2012). In the US Western Interior Basin, the lower/middle and middle/upper Campanian boundaries are marked by ammonites (Cobban *et al*. 2006). In Europe the base of the US middle Campanian substage is within the lower portion of the '*Inoceramus*' *azerbaydjanensis*–'*Inoceramus*' *vorhelmensis* Zone, proposed for the lower part of the European upper Campanian (Walaszczyk 1997; Walaszczyk *et al*. 2008), whereas the US middle/upper Campanian boundary is placed in Europe at the base, or within the '*Inoceramus*' *tenuilineatus* Zone (Walaszczyk 2004; Ogg and Hinov 2012). Using calcareous plankton biostratigraphy, the base of the upper Campanian may correspond to the base of nannofossil subzones UC15a, UC15b or UC15c (e.g., Burnett 1998) and to the base of the classical *Globotruncana ventricosa* planktonic foraminifera biozone, a concept that was strongly questioned by Petrizzo *et al*. (2011).

The Campanian/Maastrichtian boundary is defined by a ratified GSSP for the base of the Maastrichtian in a quarry at the vicinity of the village of Tercis, SW France, as the arithmetic mean of twelve bioevents including first and last occurrences of ammonites, inoceramid bivalves, planktonic and benthic foraminifera, dinoflagellate cysts and calcareous nannofossils

(Odin and Lamaurelle 2001; Ogg and Hinnov 2012). The base of the Maastrichtian was correlated to the last appearance of the nannofossil *Uniplanarius trifidus* (Stradner in Stradner and Papp) Hattner and Wise in Wind and Wise, 1983 (formerly *Quadrum trifidum* of e.g., Perch-Nielsen 1979) at the GSSP section of Tercis (Odin and Lamaurelle 2001) and later on in Tethyan zonations (e.g., Thibault *et al*. 2016). The UC16b^{TP} subzone, according to Thibault *et al.* (2016, p. 64), emends the UC16/UC17 zonation given by Burnett (1998) and redefines the (standard) nannofossil marker succession around the base of the Maastrichtian. However, at Tercis, the LO of *Uniplanarius trifidus* was not consistently reported by different nannofossil workers (Odin 2001), and positioned some 19 m below the Golden Spike point in Odin and Lamaurelle (2001), thus giving a higher range of uncertainty for correlation with the Maastrichtian GSSP.

RESULTS

Calcareous nannofossils

In general, the preservation of calcareous nannofossils is rather poor to very poor, with diagenetic overgrowth dominantly in the lower interval of the section, and additional dissolution and etching of nannofossils in the upper, siliciclastic, turbiditic part of the section (Text-fig. 4). The abundances of nannofossils are low to very low, from a maximum average of 8 specimens per field of view (FOV) to 1 specimen per 30 FOV; one sample was barren (Text-fig. 5). Low abundances and poor preservation are regarded responsible for the low diversity of these Upper Cretaceous assemblages, with a maximum of thirty-one taxa (see Appendix 1 for alphabetical list of calcareous nannofossil taxa from the Petrich section), as compared to reports of more than forty to fifty from other Santonian–Campanian assemblages (e.g., Püttmann and Mutterlose 2021).

Dinoflagellate cysts

Dinoflagellate cysts have a comprehensive record through the middle and upper part of the sampled interval in the Petrich section (from bed 12 upwards) with more than 50% palynologically positive samples. The dinocyst species diversity is moderate, with thirty documented species. Terrestrial palynomorphs are poorly represented with the occurrence of 1–2 taxa in productive samples from the upper part of the sampled interval.

Samples from P-6 to P-17, corresponding to the sampling interval beds 16–31 in the section yielded the most diverse and well preserved dinoflagellate cyst assemblages (see Appendix 2 for complete list of encountered dinoflagellate cyst taxa). *Cannosphaeropsis utinensis*, *Palaeohystrichophora infusorioides* and *Odontochitina porifera* occur already in sample P-6 and consistently range up to P-16 (Text-figs 3, 6). This dinocyst impoverished interval includes also the following species characteristic for the Campanian: *Achomosphaera crassipellis*, *A. fenestra*, *A. ramulifera*, *A. regiensis, A. sagena*, *Areoligera coronata*, *Chatangiella ditissima*, *C. tripartita*, *Corradinisphaeridium horridum*, *Exochosphaeridium majus*, *Hystrichodinium pulchrum*, *Hystrichsphaeridium duplum*, *H. salpingophorum*, *H. tubiferum*, *Isabelidinium cooksoniae*, *Oligosphaeridium complex*, *O. pulcherrimum*, *Pervosphaeridium monasteriense*, *P. pseudhystrichodinium*, *Pterodinium cingulatum*, *Raetiaedinium truncigerum*, *Spiniferites ramosus*, *S. scabrosus*, *Surculosphaeridium longifurcatum* and *Tanyosphaeridium regulare* (Text-figs 6–8). The most common dinocyst species within the assemblages are *P. cingulatum*, *O. complex*, *S. ramosus*, *C. horridum* and *C. utinensis* (Text-fig. 6). *Areoligera coronata* is represented by rare specimens and is documented in samples P-8 and P-9. Most *Chatangiella* spp. and *Isabelidinium* spp. occur in the sample set P-9 to P-15 (Text-figs 3, 6).

Palynofacies data

Palynofacies data were considered from the Campanian interval in the section. The organic matter (OM) in the samples is represented by opaque and translucent phytoclasts and dinoflagellate cysts. In the lower and middle part of the section, corresponding to samples from P-5 to P-11 (bed 12 to bed 23), the opaque phytoclasts show a very high proportion together with abundant dinoflagellate cysts. Opaque phytoclasts are typically equidimensional, rarely lath and of medium size. The interval contains also rare translucent phytoclasts of small size and equidimentional shape.

Upwards, within samples P-12 to P-22, corresponding to the interval from bed 24 to bed 37, a slight change occurs in the palynofacies composition (Text-fig. 9). The proportion of opaque phytoclasts and dinocysts decreases slightly and large translucent structured phytoclasts, such as woody tissues and cuticles, appear in the palynofacies. The continental input increases upwards in this interval with structured translucent phytoclasts and spores. Samples P-14, P-21 and P-24 include moderate content of

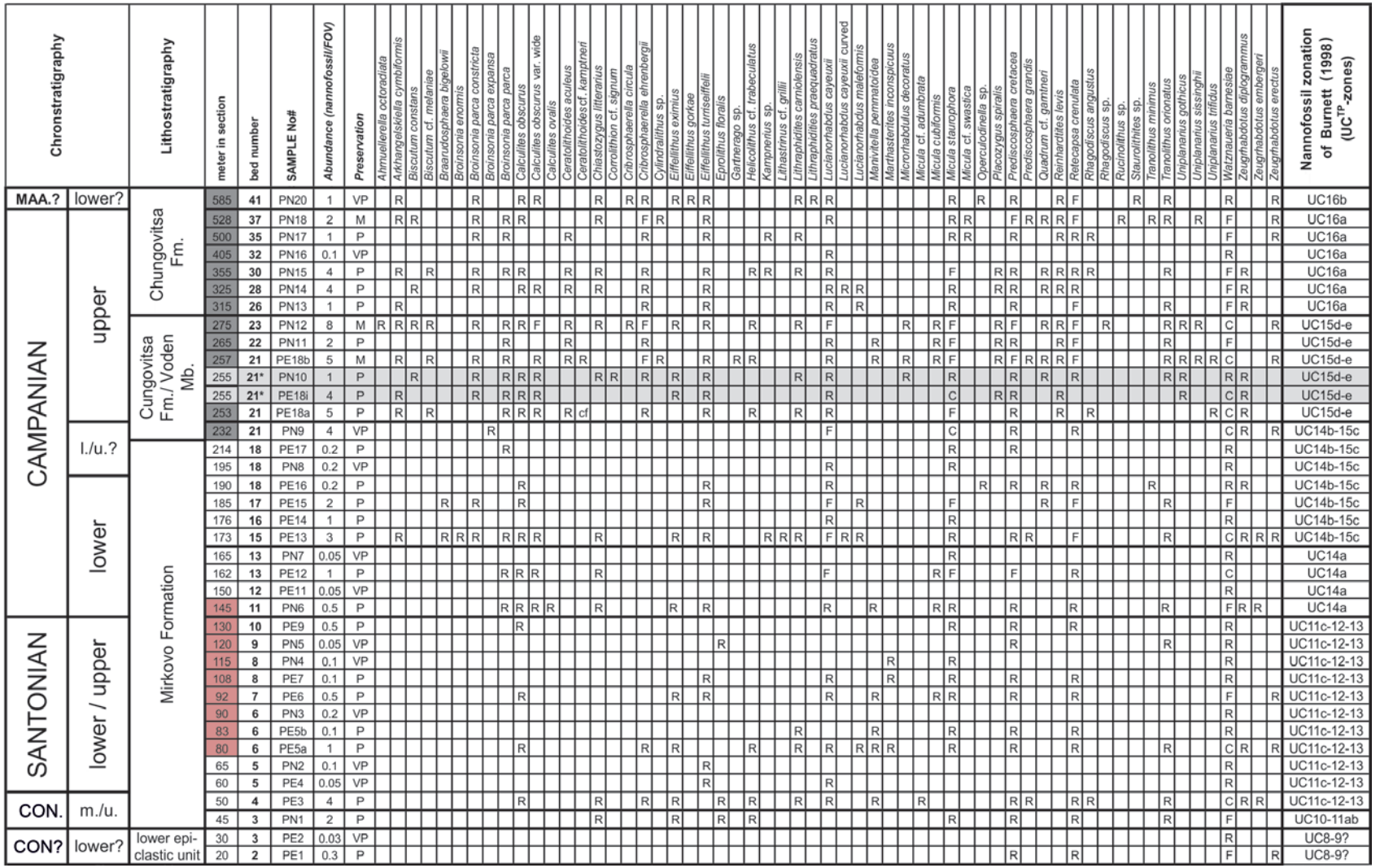

Text-fig. 5. Range chart of nannofossil species and nannofossil zones of Burnett (1998) identified in the Petrich section, with lithostratigraphy and meter in section (see Text-fig. 3 for details); red limestone interval marked in red; turbiditc-shale interval marked in dark grey. Inoceramid-bearing bed marked in light grey and with an asterisk.Total sample abundance estimates are given by nannofossils per field of view (FOV). Preservation: VP – very poor (overgrowth and dissolution hinder species or even genus identification of more than 50% of the nannofossil remains, only most solution resistant species present), P – poor (genus identification of most nannofossils possible, but delicate forms are missing), M – medium (most nannofossils can be identified to genus and species level).

Individual taxon abundance is classified as: C – common (more than 1 specimen per FOV), F – few (more than 1 specimen per 10 FOVs), R – rare (less than 1 specimen per 10 FOVs).

C A M P A N I A N										Chronostratigraphy
M. Fm.	Chungovitsa Fm. / Voden Member					Chungovitsa Fm.				Lithostratigraphy
176	220	240	260	270	280	290	300	320	370	meter in section
16	19	21	21	22	23	24	26	27	31	bed number
P-6	P-7	P-8	P-9	P-10	P-11	P-12	P-13	P-14	P-16	SAMPLE №
	R	R	R							*Achomosphaera crassipellis*
	C	C	R	C				C		*Achomosphaera fenestra*
	C	R	R							*Achomosphaera ramulifera*
	C	R	C			R				*Achomosphaera sagena*
		R	R							*Areoligera coronata*
R	R	C	R					C	R	*Cannosphaeropsis utinensis*
			R	R					R	*Chatangiella ditissima*
			R	R						*Chatangiella tripartita*
		C			C	C				*Corradinisphaeridium horridum*
	R	R					R			*Exochosphaeridium majus*
	C	R	C		R					*Hystrichodinium pulchrum*
		R		R		R				*Hystrichosphaeridium duplum*
										Hystrichodinium pulchrum
	C	C		R	R	C			C	*Hystrichosphaeridium salpingophorum*
	C	C		R	R	C	R		R	*Hystrichosphaeridium tubiferum*
					R			R		*Isabelidinium cooksoniae*
R	R	R							R	*Odontochitina porifera*
	C	C							C	*Oligosphaeridium complex*
		R	R					R		*Oligosphaeridium pulcherrimum*
R	R	R	R					R	R	*Palaeohystrichophora infusorioides*
				R	R					*Pervosphaeridium monasteriense*
				R	R					*Pervosphaeridium pseudhystrichodinium*
	C	C	R		C	C		C	C	*Pterodinium cingulatum*
				R	R					*Raetiaedinium truncigerum*
	R							R		*Spiniferites membranaceus*
R	C	C		C	C		R	C	C	*Spiniferites ramosus*
		R	R							*Spiniferites scabrosus*
		C			C	R				*Surculosphaeridium longifurcatum*

Text-fig. 6. Quantitative range chart of dinoflagellate cyst species from the Campanian interval in the Petrich section, Bulgaria. Abundance of species is classified as R – rare (1–9 specimens), C – common (10–20 specimens), A – abundant (more than 20 specimens).

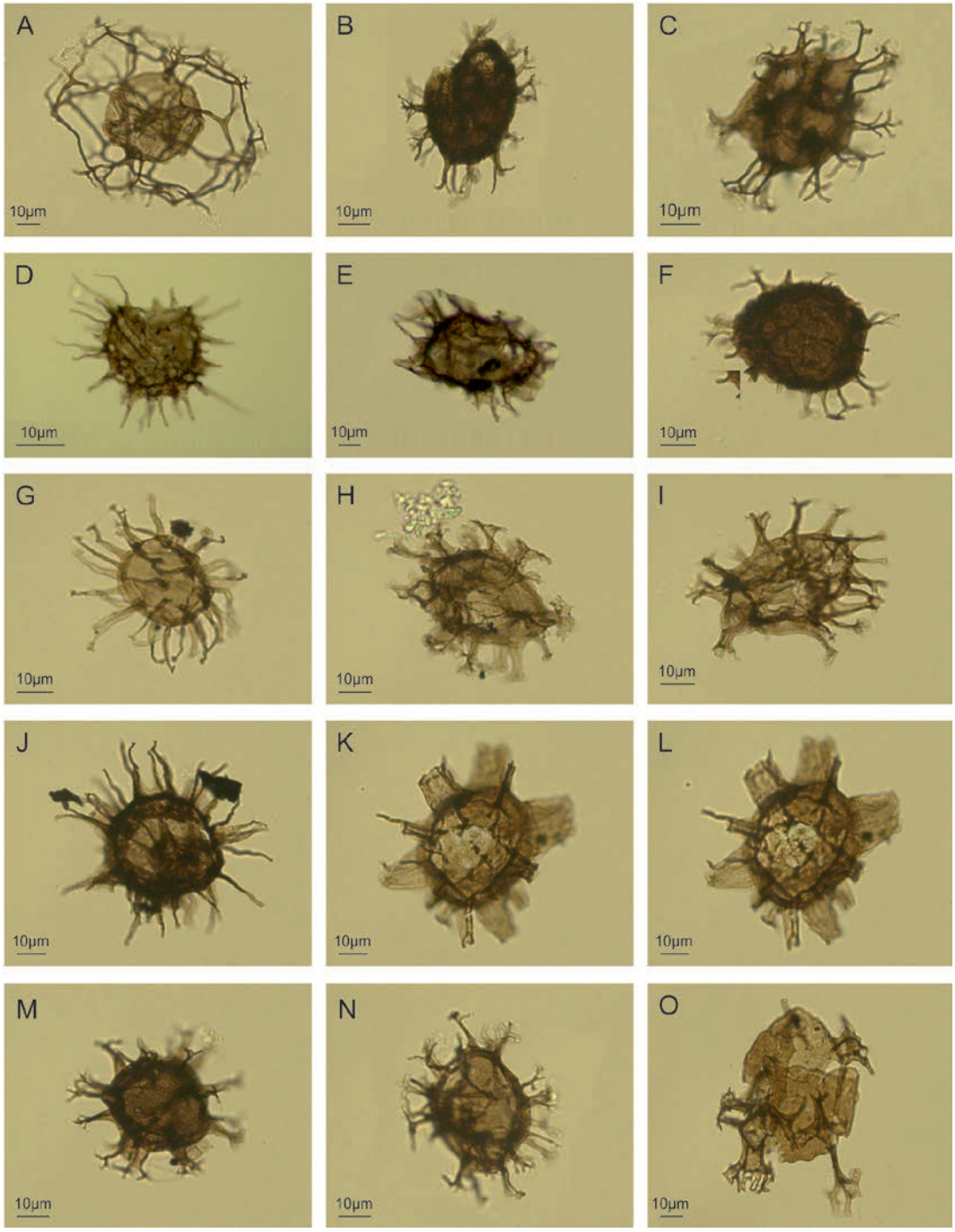

Text-fig. 7. Microphotographs of characteristic dinoflagellate cyst species from the Petrich section, Bulgaria. **A** – *Cannosphaerosis utinensis* Wetzel, 1933, sample P-8, bed 21. **B** – *Achomosphaera fenestra* Kirsch, 1991, sample P-11, bed 23. **C** – *Achomosphaera ramulifera* (Deflandre) Evitt, 1963, sample P-8, bed 21. **D** – *Hystrichodinium pulchrum* Deflandre, 1935, sample P-8, bed 21. **E** – *Corradinisphaeridium horridum* (Deflandre) Masure, 1986, sample P-8, bed 21. **F** – *Achomosphaera sagena* Davey and Williams, 1966, sample P-7, bed 19. **G** – *Hystrichosphaeridium duplum* Lentin and Williams, 1989, sample P-11, bed 23. **H** – *Hystichosphaeridium salpingophorum* (Deflandre) Deflandre, 1937, sample P-11, bed 23. **I** – *Hystrichosphaeridium tubiferum* (Ehrenberg) Deflandre, 1937, sample P-8, bed 21. **J** – *Pervosphaeridium pseudhystricodinium* (Deflandre) Yun, 1981, sample P-7, bed 19. **K**, **L** – *Raetiaedinium truncigerum* (Deflandre) Kirsch, 1991, sample P-10, bed 22; K – high focus, L – low focus. **M** – *Spiniferites scabrosus* (Clarke and Verdier) Lentin and Williams, 1975, sample P-8, bed 21. **N** – *Spiniferites ramosus ramosus* (Ehrenberg) Davey and Williams, 1966, sample P-7, bed 19. **O** – *Oligosphaeridium pulcherrimum* (Deflandre and Cookson) Davey and Williams, 1966, sample P-14, bed 27. All photomicrographs were taken using transmitted light microscopy. For position of samples in section see Text-fig. 3.

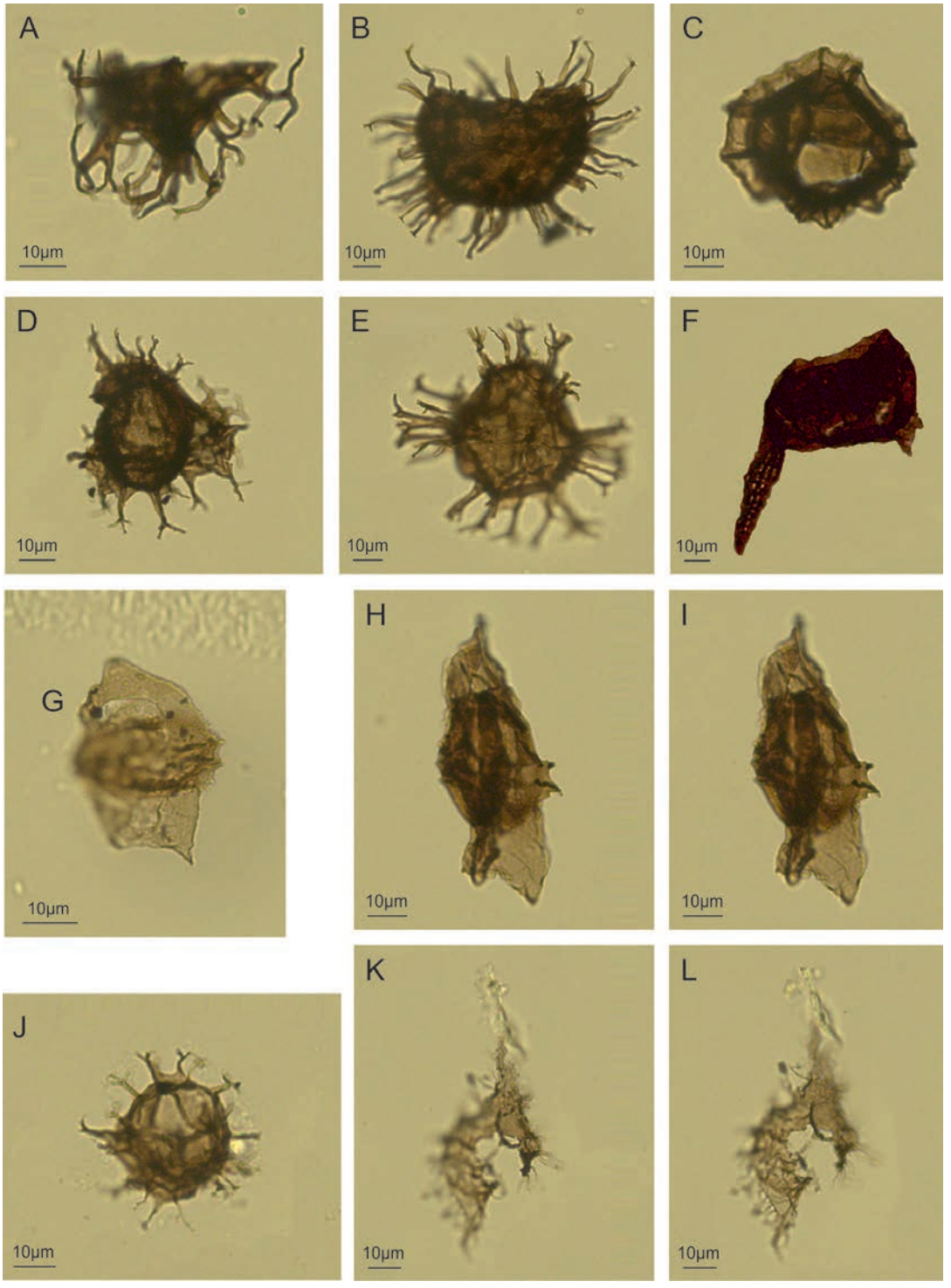

Text-fig. 8. Microphotographs of characteristic dinoflagellate cyst species from the Petrich section, Bulgaria. **A –** *Areoligera* cf. *coronata* (Wetzel) Lejeune-Carpentier, 1938, sample P-8, bed 21. **B –** *Exochosphaeridium majus* (Lejeune-Carpentier) Peyrot, 2011, sample P-7, bed 19. **C –** *Pterodinium cingulatum* (Wetzel) Below, 1981, sample P-14, bed 27. **D –** *Spiniferites membranaceus* (Rossignol) Sarjeant, 1970, sample P-7, bed 19. **E –** *Spiniferites* sp., sample P-7, bed 19. **F –** *Odontochitina porifera* Cookson, 1956, sample P-8, bed 21. **G –** *Chatangiella ditissima* (McIntyre) Lentin and Williams, 1976, sample P-10, bed 22. **H**, **I –** *Chatangiella tripartita* (Cookson and Eisenack) Lentin and Williams, 1976, sample P-10, bed 22; H – high focus, I – low focus. **J –** *Achomosphaera crassipellis* (Deflandre and Cookson) Stover and Evitt, 1978, sample P-8, bed 21. **K**, **L –** *Palaeohystrichophora infusorioides* Deflandre, 1935, sample P-8, bed 21; K – high focus, L – low focus. All photomicrographs were taken using transmitted light microscopy. For position of samples in section see Text-fig. 3.

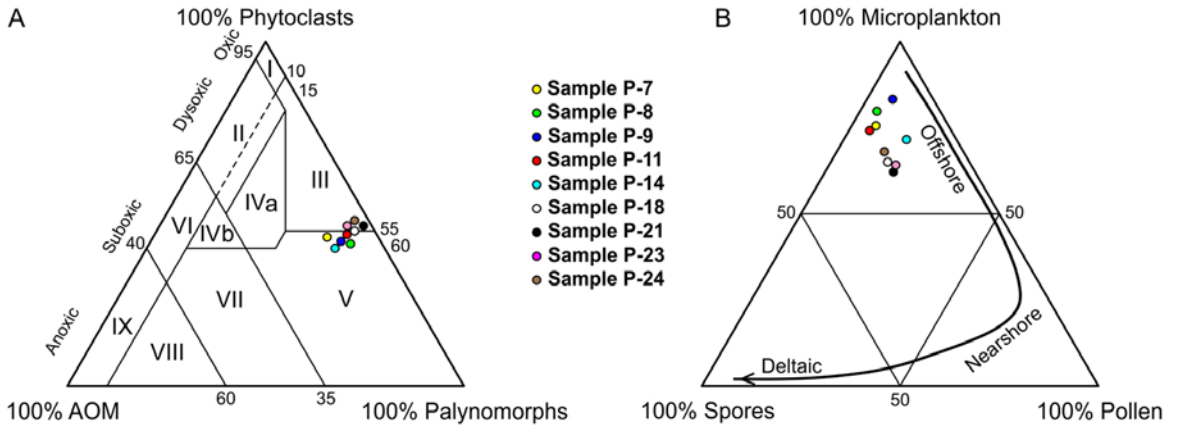

Text-fig. 9. Ternary kerogen and palynomorph plots of the Campanian interval in the Petrich section, Bulgaria. A – AOM–Phytoclast–Palynomorph plot of Tyson (1993). Field V indicates a distal oxic shelf. B – Microplankton–Spore–Pollen ternary plot (after Fedorova 1977 and Duringer and Doubinger 1985).

Text-fig. 10. '*Inoceramus*' *agdjakendsis* Aliev, 1952, U.S., K_2 1809, from the Voden Member of the Chugovitsa Formation, Petrich section, Bulgaria.

terrestrial palynomorphs and spores, belonging to *Verrucosisporites* spp. and *Cyathidites* spp.

Inoceramid bivalves

The described and herein illustrated inoceramid fauna is the first inoceramid record established from Campanian strata of the Panagyurishte strip. All specimens were obtained from a single level of light grey to grey marlstones, belonging to the upper part of bed 21 (Text-fig. 3), which is a part of the Voden Member of the Chugovitsa Formation.

The collected inoceramid assemblage is dominated by medium- to large-sized representatives of *Cataceramus* spp., *Cordiceramus* spp., *Sphaeroceramus* spp. and '*Inoceramus*' spp. (Text-figs 10–17). The described and discussed taxa are as follows: *Cataceramus ellipticus* (Giers, 1964), *Cataceramus pteroides* (Giers, 1964), *Cataceramus* ex gr. *balticus* (Böhm, 1907), *Cataceramus* sp. A, *Cataceramus* sp., *Cordiceramus* sp., '*Inoceramus*' *agdjakendsis* Aliev, 1952 and *Sphaeroceramus sarumensis* (Woods, 1911).

BIOSTRATIGRAPHY

Nannofossil zonation and age assessment
(Text-fig. 5)

Nannofossil zones UC10–UC11ab

The two lowermost samples of the Petrich section (PE-1, PE-2) yielded only solution resistant nannofossils like *Watznaueria barnesae* (Black) Perch-

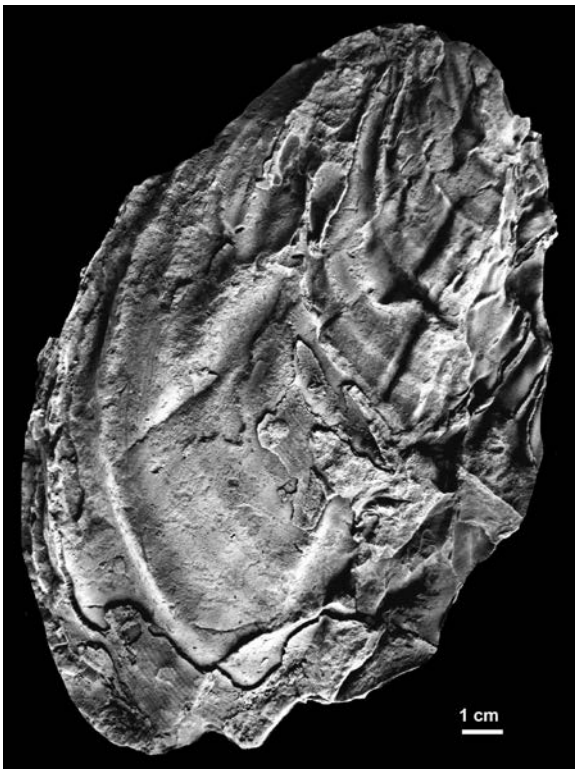

Text-fig. 11. '*Inoceramus*' *agdjakendsis* Aliev, 1952, U.S., K_2 1810, from the Voden Member of the Chugovitsa Formation, Petrich section, Bulgaria.

Nielsen, 1968, *Prediscosphaera cretacea* (Arkhangelsky) Gartner, 1968, and *Retecapsa crenulata* (Bramlette and Martini) Grün in Grün and Allemann, 1975, which have only poor biostratigraphic utility. The first biostratigraphically interpretable sample (PN-1) from bed 3 included *Micula staurophora* (Gardet) Stradner, 1963, whose FO defines nannofossil zone UC10 and starts in the middle Coniacian (Burnett 1998). Due to the low abundance and the poor preservation, the absence of other, more delicate, dissolution prone and generally rare (subzonal) markers like *Lithastrinus grillii* Stradner, 1962, and *Quadrum gartneri* Prins and Perch-Nielsen in Manivit *et al*., 1977*,* cannot be used for further biostratigraphic subdivision. Therefore, sample PN-1 can be assigned to a broader interval of nannofossil zones UC10–UC11ab. This interval spans the middle to upper Coniacian (Burnett 1998).

Nannofossil zones UC11c–UC13

The next sample interval starts with bed 4 (sample PE-3) up to bed 10 (PE-9) and includes the lower to middle part of the red limestone interval (Mirkovo Fm.) in the Petrich section. This interval is characterized by the co-occurrence of *Micula staurophora* with *Lucianorhabdus cayeuxii* Deflandre, 1959 and *Calculites obscurus* (Deflandre) Prins and Sissingh in Sissingh, 1977. The FO of *L. cayeuxii* defines the base of UC11c. Together with the common occurrence of *C. obscurus* this suggests a late Coniacian age (Burnett 1998). However, the following zonal marker *Lithastrinus septenarius* Forchheimer, 1972 (whose LO defines the base of UC12) was not found, and the marker *Arkhangelskiella cymbiformis* Vekshina, 1959 (Text-fig. 4A; its FO defines the base of UC13) occurs only sporadically in higher samples of the Petrich section above UC14. Therefore, these zones define only a broad interval from the uppermost Coniacian to upper Santonian. In addition, *Marthasterites inconspicuus* Deflandre, 1959, is present within this interval.

Nannofossil zone UC14a

The FO of *Broinsonia parca parca* (=*Aspidolithus parcus parcus* of other authors, e.g., Miniati *et al.* 2020) in sample PN-6 defines the base of zone UC14 and the base of subzone UC14a (Burnett 1998). This bioevent is recorded in bed 11 (at c. 145 m) of the Petrich section, near the top of the red limestone interval. At the same level, the FO of *Calculites obscurus* with a wide central longitudinal suture is noted, which was reported by Wolfgring *et al.* (2018) as starting just below the FO of *B. parca parca*. Both bioevents bracket the base of the Campanian as defined by the base of Chron C33r (Wolfgring *et al.* 2018) with *B. parca parca* starting slightly above the Santonian/Campanian boundary.

Nannofossil zone UC14b^{TP}–UC15c^{TP}

The FO of *Broinsonia parca constricta* Hattner, Wind and Wise, 1980 in sample PE-13 (= *Aspidolithus parcus constrictus*; e.g., Miniati *et al.* 2020) defines the base of UC14b in the Tethyan–Intermediate province zonation of the lower Campanian (Burnett 1998). However, other following bioevents are missing in the Petrich section, e.g., the successive FOs of *Bukryaster hayi* (Bukry) Prins and Sissingh in Sissingh, 1977, *Ceratolithoides verbeeki* Perch-Nielsen, 1979, and *Monomarginatus pleniporus* Wind and Wise in Wise and Wind, 1977, or are higher up in the section and do not follow the defined stratigraphic succession as noted for *Ceratolithoides aculeus* (Stradner) Prins and Sissingh in Sissingh, 1977, and *Uniplanarius*

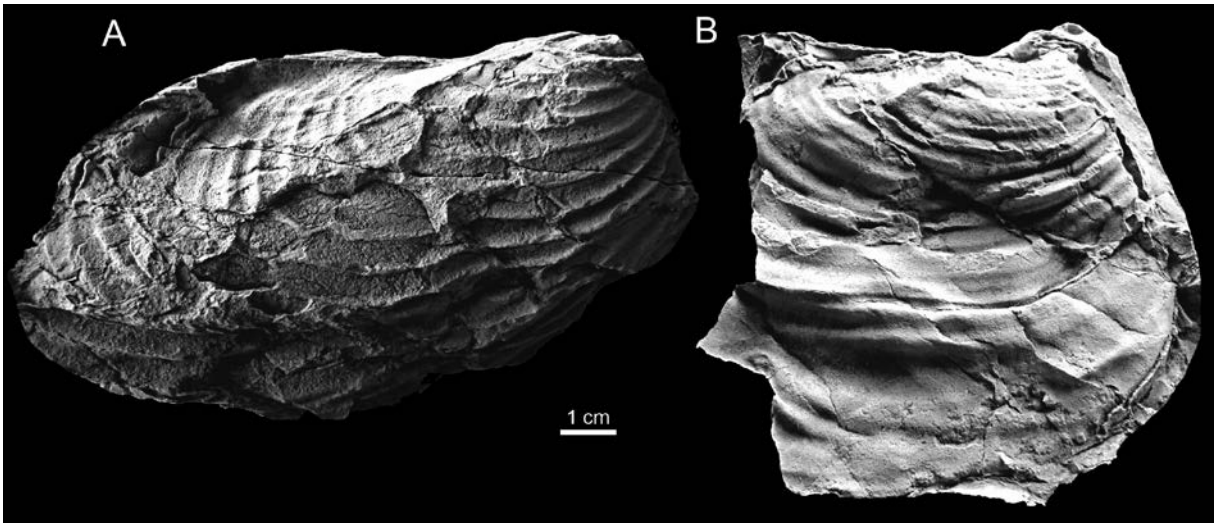

Text-fig. 12. Campanian inoceramid bivalves from the Voden Member of the Chugovitsa Formation, Petrich section, Bulgaria. **A** – *Cataceramus ellipticus* (Giers, 1964), U.S., K_2 1829. **B** – *Cataceramus* ex gr. *balticus* (Böhm, 1907), U.S., K_2 1830.

sissinghii (Perch-Nielsen) Farhan 1987. Therefore, this interval can only be very generally assigned to the interval of UC14b^{TP} to UC15c^{TP}, which spans the lower to upper Campanian boundary (Burnett 1998). Consequently, this interval ranges from the upper lower Campanian to the lower upper Campanian using a twofold subdivision of the Campanian.

Nannofossil zone UC15d^{TP}–UC15e^{TP}

The FO of *Uniplanarius trifidus* in sample PE-18a (bed 21, at 253 m; Text-fig. 4O) defines the base of UC15d of the Tethyan–Intermediate (^{TP}) province zonation of Burnett (1998), and occurs in the inoceramid bed described below. This interval is assigned to the lower part of the upper Campanian according to Burnett (1998). *Reinhardtites levis* Prins and Sissingh in Sissingh, 1977, and *Ceratolithoides aculeus* have also their FOs within the same sample, which apparently is a sign of some preservational bias, as these marker species should have been present already below this interval (see Burnett 1998). Within the range of *U. trifidus* also rare specimens of *Ceratolithoides kamptneri* Bramlette and Martini, 1964, are found. The top of this interval is defined by the last regular occurrence of *Eiffellithus eximius* (Stover) Perch-Nielsen, 1968, the LO of which marks the base of UC16, whereas the Santonian–Campanian marker *Reinhardtites anthophorus* (Deflandre) Perch-Nielsen, 1968, is totally missing from the Petrich section.

Nannofossil subzone UC16a^{TP}

Uniplanarius trifidus is extremely rare (only found in 2 samples), therefore we use the LO of *Uniplanarius sissinghii* in bed 37 in bed 37 (sample PN-18, 528 m) as an alternative marker for the top of subzone UC16a^{TP} as emended by Thibault *et al*. (2016). This subzone marks the upper part of the upper Campanian according to Thibault *et al*. (2016).

Nannofossil subzone UC16b^{TP}

The presence of *Reinhardtites levis* and *Tranolithus orionatus* (Reinhardt) Reinhardt, 1966, together with *Broinsonia parca constricta*, but without any *Uniplanarius* spp. in sample PN-20 indicates subzone UC16b^{TP} of Thibault *et al*. (2016) and marks the base of the Maastrichtian in the interval between PN-18 (528 m) and the topmost sample PN-20 (bed 41 at 585 m). However, due to the poor preservation with some dissolution and etching in this turbiditic interval, the presence/absence data may show some bias, and further work is needed to assure the base of the Maastrichtian in the Petrich section.

Dinocyst biostratigraphy

The present study provides detailed and calibrated dinocyst data in the discussed stratigraphic interval. The outlined dinocyst succession is new and first reported from Bulgaria.

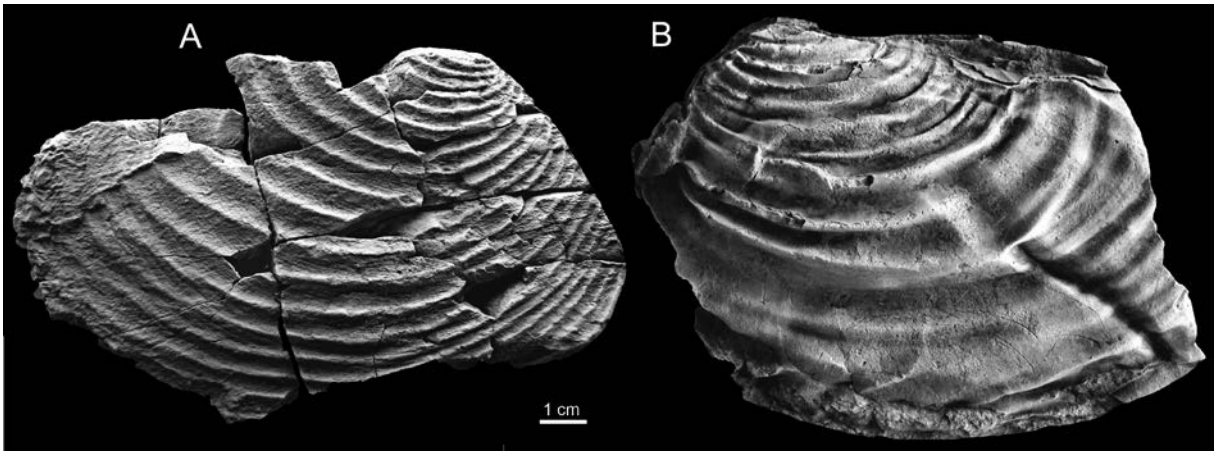

Text-fig. 13. Campanian inoceramid bivalves from the Voden Member of the Chugovitsa Formation, Petrich section, Bulgaria. **A** – *Cordiceramus* sp., U.S., K_2 1818. **B** – *Cataceramus pteroides* (Giers, 1964), U.S., K_2 1819.

Biostratigraphic interpretations are based on comparisons with several previous dinocyst studies in Europe, namely in the Campanian historical stratotype section at Charente in France (Masure 1985), the Maastrichtian type area in Limburg (Robaszynski *et al.* 1985; Slimani 2001, 2011), the GSSP for the base of the Maastrichtian at Tercis les Bains in France (Antonescu *et al*. 2001; Schiøler and Wilson 2001), northern Spain (Radmacher *et al.* 2014), the Campanian in Bavaria (Kirsch 1991), Austria (Mohamed and Wagreich 2013), Czech Republic (Skupien and Mohamed 2008), south-eastern Poland (Niechwedowicz and Walaszczyk 2022; Slimani *et al.* 2021), as well as Italy (Corradini 1973; Roncaglia and Corradini 1997; Roncaglia 2002), and regions of the Northern Hemisphere (Stover *et al.* 1996; Williams *et al.* 2004).

Based on these correlations it can be concluded that some taxa, such as *Achomosphaera fenestra*, *Areoligera coronata*, *Cannosphaeropsis utinensis*, *Chatangiella ditissima*, *Chatangiella tripartite*, *Corradinisphaeridium horridum*, *Hystrichodinium pulchrum*, *Odontochitina porifera*, *Palaeohystrichophora infusorioides*, *Pervosphaeridium pseudhystrichodinium* and *Raetiaedinium truncigerum* appear to have a similar distribution pattern and thus may prove important interregional marker species. These taxa and their concurrent range have been estimated as key markers for the Campanian on a wide geographic scale.

The entire dinocyst assemblage from the Petrich section points to the Campanian. *Cannosphaeropsis utinensis* appears in the latest Santonian (Williams *et al*. 2004), and *Achomosphaera fenestra*, *A. regiensis* and *Areoligera coronata* in the earliest Campanian (Kirsch 1991). According to Kirsch (1991), the FO of *Corradinisphaeridium horridum* is a good proxy for the middle Campanian. The species has its LO roughly at the Campanian–Maastrichtian boundary (Antonescu *et al.* 2001; Schiøler and Wilson 2001; Mohamed and Wagreich 2013; Radmacher *et al.* 2014), similarly as *Raetiaedinium truncigerum* (Antonescu *et al.* 2001; Slimani 2001). A good proxy for the upper part of the upper Campanian is the LO of *Odontochitina porifera* (Niechwedowicz and Walaszczyk 2022), also considered to represent a potential marker for the Campanian–Maastrichtian boundary (CMB) in the type boundary section at Tercis, southwest France (Schiøler and Wilson 2001), as well as in Zumaia, northern Spain (Radmacher *et al*. 2014). In the Petrich assemblages, important Campanian markers are also *Chatangiella ditissima* and *C. tripartita*. Most species of the genus *Chatangiella* Vozzhennikova, 1967 disappear during the late Campanian in the Northern Hemisphere, according to Vozzhennikova (1967) and Slimani (2021).

The encountered dinocyst association indicates the *Areoligera coronata* Zone *sensu* Kirsch (1991) in the Petrich section with a stratigraphical range from the upper part of the lower Campanian to the upper Campanian and direct calibration to the nannofossil subzones UC14b^{TP}–UC16a^{TP}. The zone is indicated both, by the presence of the index species, but also by the characteristic zonal association and concurrent range of *Achomosphaera fenestra*, *Areoligera coronata*, *Cannosphaeropsis utinensis*, *Chatangiella ditissima*, *C. tripartita*, *Corradinisphaeridium horridum*, *Hystrichodinium pulchrum*, *Odontochitina porifera*, *Palaeohystrichophora infusorioides*, *Pervo-*

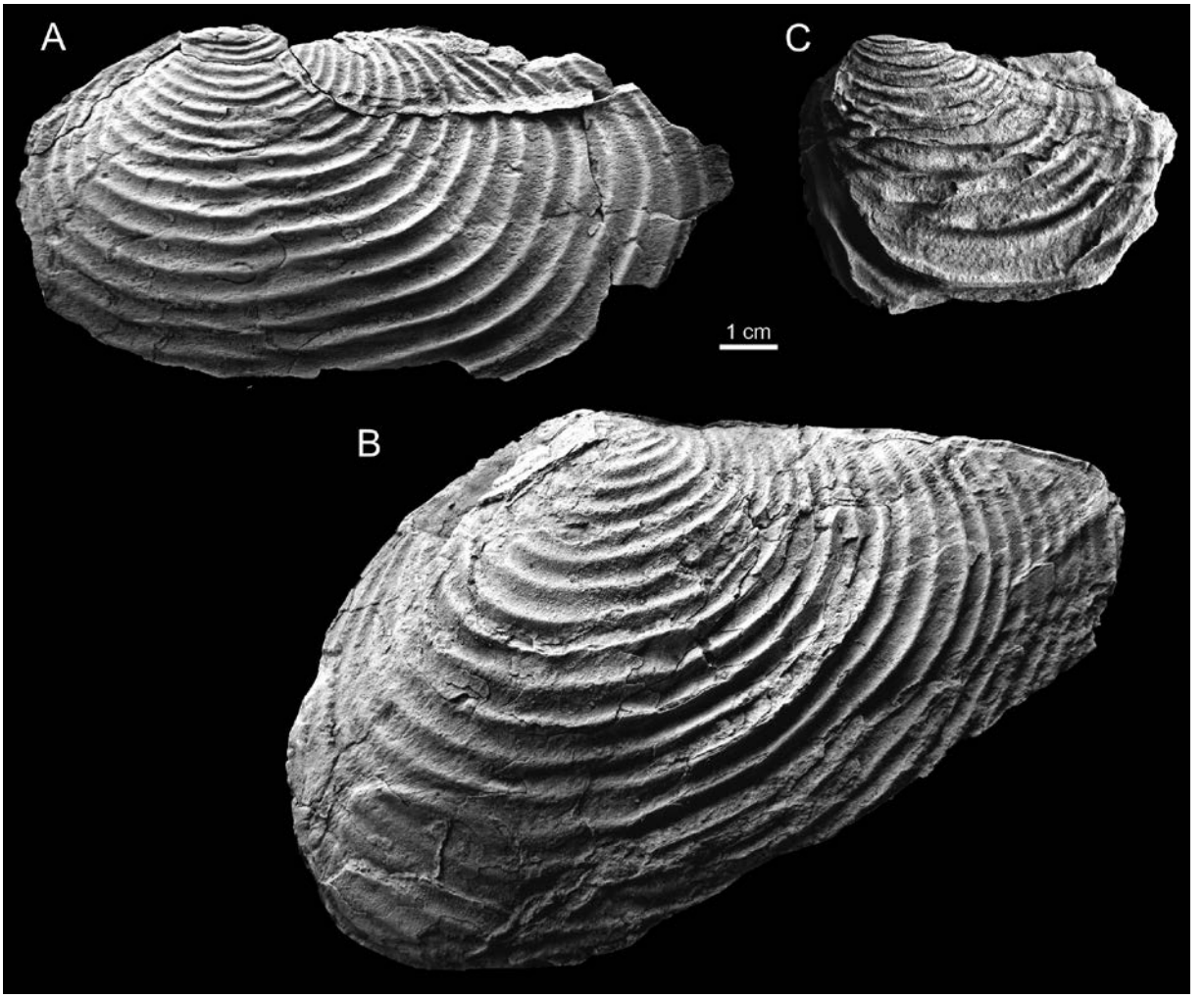

Text-fig. 14. Campanian inoceramid bivalves from the Voden Member of the Chugovitsa Formation, Petrich section, Bulgaria. **A**, **B** – *Cataceramus* sp., A – U.S., K_2 1820; B – U.S., K_2 1821. **C** – *Cataceramus pteroides* (Giers, 1964), U.S., K_2 1822.

sphaeridium monasteriense, *P. pseudhystrichodinium* and *Raetiaedinium truncigerum* (see Text-fig. 3).

Inoceramid biostratigraphy

During the Late Cretaceous, inoceramid bivalves were distributed worldwide and had a rapid rate of evolution, therefore inoceramid assemblages provide a powerful tool for a refined biostratigraphy in the Cenomanian through to middle Maastrichtian strata. In the last two decades, the knowledge about the taxonomy, biozonation and high correlation potential of Campanian and Campanian–Maastrichtian inoceramid records has been greatly enriched (Walaszczyk 1997, 2004; Walaszczyk *et al*. 2001, 2002a, b, 2008, 2014; Jagt *et al*. 2004; Walaszczyk and Dhondt 2005; Kennedy *et al*. 2007; Jurkowska 2016). Moreover, a detailed inoceramid stratigraphy and biozonation was proposed and widely accepted for the Campanian stage (Walaszczyk 1992, 1997, 2004; Walaszczyk *et al*. 2008).

In Bulgaria, the Campanian inoceramid record is relatively poorly known, excluding uppermost Campanian inoceramid faunas recorded mainly from the Western Fore-Balkan Mountains (northwestern Bulgaria) (Jolkičev 1962; Tsankov 1981; Dochev *et al*. 2018; Pavlishina *et al*. 2020). It should be noted that inoceramids collected from the Eastern Fore-Balkan Mountains, previously recorded by Jolkičev (1962), and referred to as Maastrichtian in age, were revised and recognized as late Campanian (see Walaszczyk 1997 and Walaszczyk *et al*. 2002).

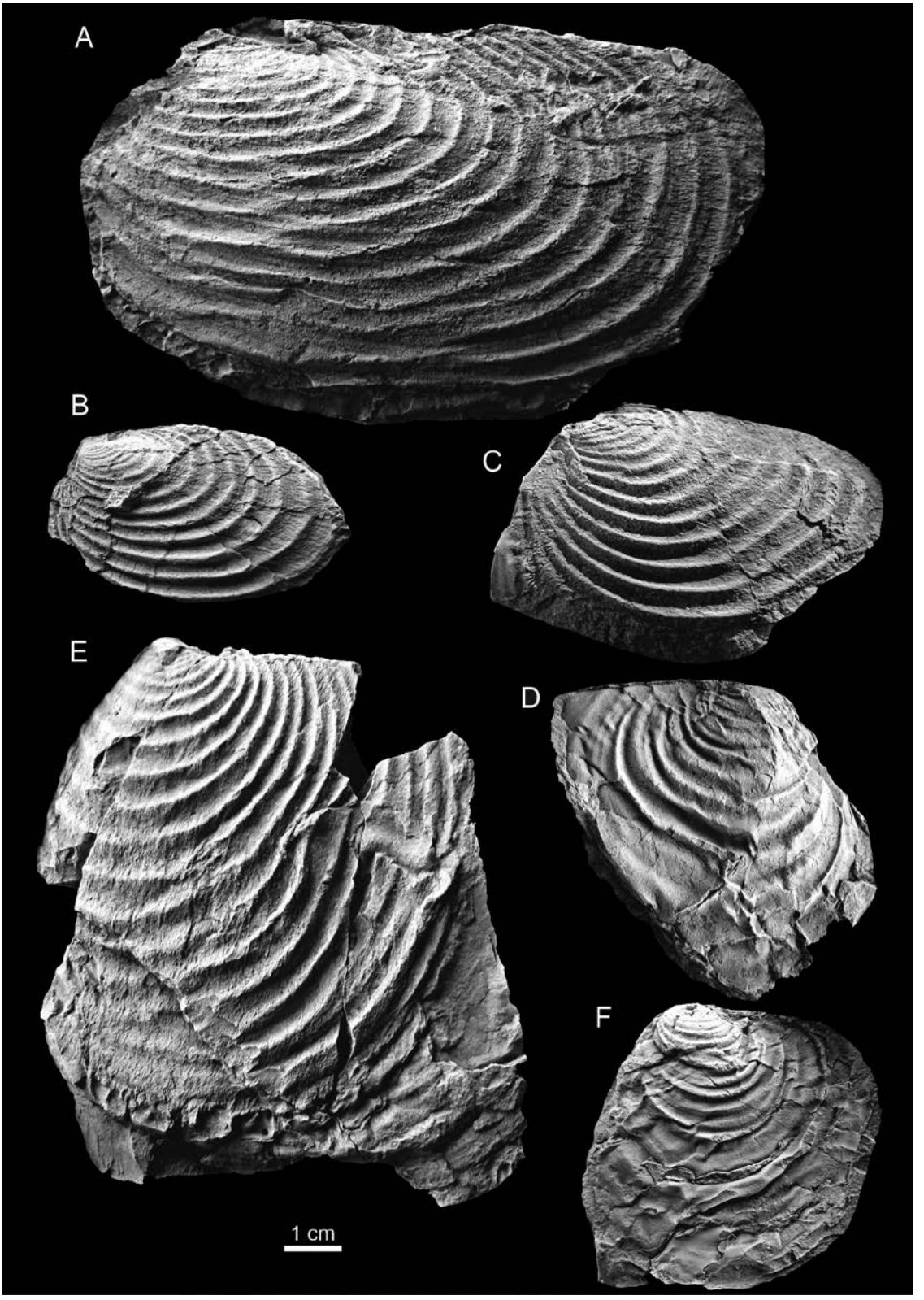

Text-fig. 15. Campanian inoceramid bivalves from the Voden Member of the Chugovitsa Formation, Petrich section, Bulgaria. **A** – *Cordiceramus* sp., U.S., K_2 1812. **B**, **C**, **E** – *Cataceramus* sp., B – U.S., K_2 1813; C – U.S., K_2 1814; E – U.S., K_2 1816. **D**, **F** – *Cataceramus* sp. A, D – U.S., K_2 1815; F – U.S., K_2 1817.

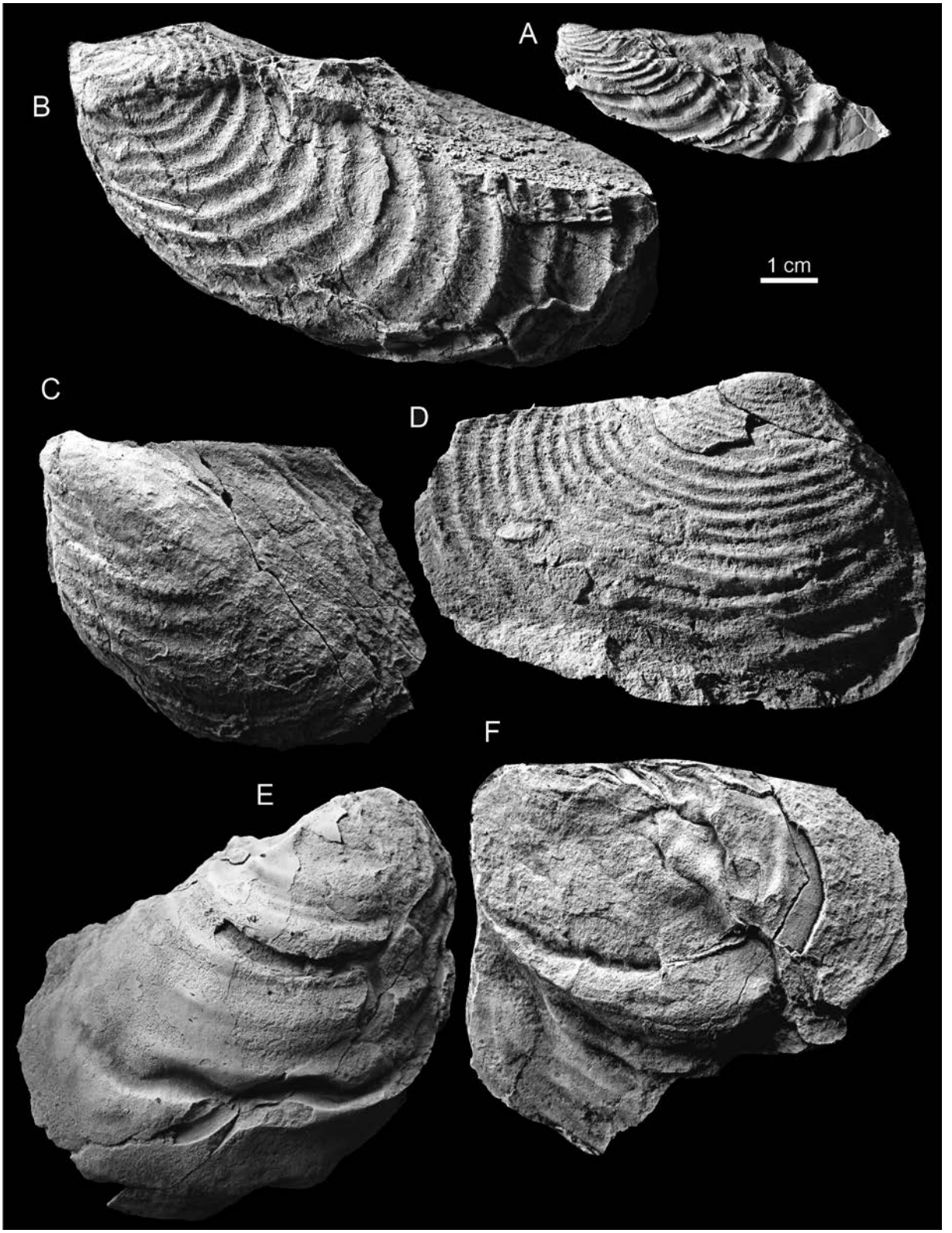

Text-fig. 16. Campanian inoceramid bivalves from the Voden Member of the Chugovitsa Formation, Petrich section, Bulgaria. **A**, **B**, **D** – *Cataceramus* sp., A – U.S., K_2 1823; B – U.S., K_2 1824, D – U.S., K_2 1826. **C**, **F** – '*Inoceramus*' sp., C – U.S., K_2 1825; F – U.S., K_2 1828. **E** – *Sphaeroceramus sarumensis* (Woods, 1911), U.S., K_2 1827.

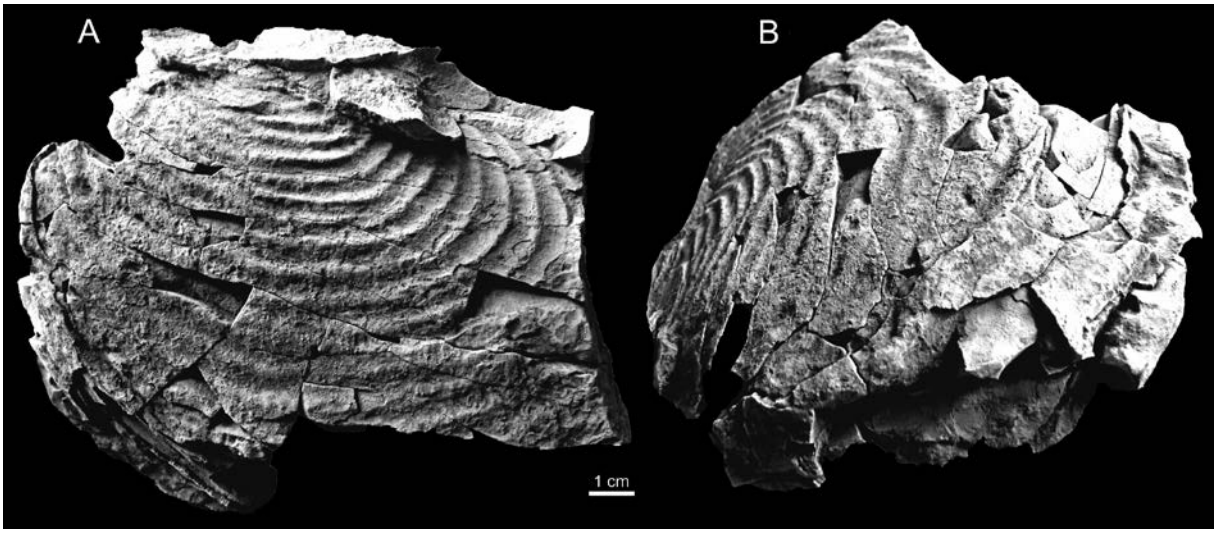

Text-fig. 17. *Cataceramus* ex gr. *balticus* (Böhm, 1907), U.S., K_2 1811, from the Voden Member of the Chugovitsa Formation, Petrich section, Bulgaria, A – top view, B – oblique lateral view.

The collected inoceramid assemblage from the Petrich section contains strongly oblique specimen of '*Inoceramus*' *agdjakendsis* (Text-figs 10, 11), *Cataceramus ellipticus* (Text-fig. 12A), and *Cataceramus pteroides* (Text-figs 13B and 14C), all characteristic for the '*Inoceramus*' *azerbaydjanensis* – '*Inoceramus*' *vorhelmensis* Zone, recognized in the lower Upper Campanian (according to the European stage subdivision) as proposed by Walaszczyk (1997). The other taxa present *Cordiceramus* sp. (Text-figs 13A and 15A), *Sphaeroceramus sarumensis* (Text-fig. 16E), *Cataceramus* ex gr. *balticus* (Text-figs 12B, 17), *Cataceramus* sp. A (Text-fig. 15D, F), *Cataceramus* sp. (Text-figs 14A, B, 15B, C, E, 16A, B, D) and '*Inoceramus*' sp. (Text-fig. 16C, F) are not stratigraphically diagnostic, although *S. sarumensis* seems not to range higher. The zone was also recorded in a coeval interval of the US Western Interior (lower Middle Campanian according to the three-fold North American subdivision) (Walaszczyk *et al*. 2001). The high correlation potential of the zone (and of its inoceramid association) for the European Campanian and its trans-Atlantic correlation was later confirmed by Jagt *et al*. (2004) and Walaszczyk *et al*. (2008).

As stated above, the described '*Inoceramus*' *agdjakendsis*, *Cataceramus ellipticus* and *Cataceramus pteroides* are part of the inoceramid association characteristic for the '*Inoceramus*' *azerbaydjanensis* – '*Inoceramus*' *vorhelmensis* Zone, although the zonal taxa are missing.

CHRONOSTRATIGRAPHY

The nannofossil data from the Petrich section, although potentially biased due to the low nannofossil abundances and poor preservation, give evidence of a continuous succession of epiclastic, pelagic to turbiditic deposits from the middle/upper Coniacian (UC10, FO of *Micula staurophora*) to the Campanian–Maastrichtian boundary interval (UC16b^{TP}, above the LO of *Uniplanarius* spp.). The epiclastic base of the section, below UC10, may thus be assigned to the lower Coniacian or older. The base of the Santonian is not well defined, although two markers (*Lucianorhabdus cayeuxii* and *Calculites obscurus*) for the upper to uppermost Coniacian have a well-defined FO at bed 4 (c. 50 m) and thus define the start of the Coniacian–Santonian boundary interval. However, no other marker higher up in the section is available for further constraining the Coniacian–Santonian boundary within this not further subdivided interval of UC11c–UC13.

The base of the Campanian is well defined in the Petrich section by the first occurrence of *Broinsonia parca parca* in bed 11 (c. 145 m). Although very rare (only 2 specimens found in 500 FOV), these first specimen attributed to *B. parca parca* have a length above 9 μm, and a b/a ratio (see Gardin *et al*. 2001; Wolfgring *et al*. 2018; Miniati *et al*. 2020) of 1.3 to 1.1. A further subdivision of the Campanian into lower/middle/upper Campanian is not well defined by nannofossils within the Petrich section because of

poor preservation within the mostly reddish pelagic limestones, thus several zones or subzones have to be combined into one zone.

The base of the Maastrichtian is provisionally defined between the uppermost samples of the section (PN-18 and PN-20), between bed 37 and bed 41 (528 to 585 m). The last occurrence of *Uniplanrius* spp. and the continuous presence of *Broinsonia parca constricta* gives evidence for nannofossil subzone UC16b^{TP} (Thibault *et al*. 2016) and thus indicates the provisional base of the Maastrichtian in this topmost part of the Petrich section.

The dinocyst record of the Petrich section is assessed by direct calibration to the outlined nannofossil zonation. The stratigraphical range of the recognized *Areoligera coronata* dinocyst Zone is within the interval of nannofossil subzones UC14b^{TP}–UC16a^{TP} and has a stratigraphical range from the upper parts of the lower Campanian to the upper Campanian in the section.

Based on the nannofossil bioevents and zonation, the inoceramid level (bed 21, assigned to the lower part of the upper Campanian, based on inoceramid zonal correlation), is placed within the interval of nannofossil subzones UC15d^{TP} and UC15e^{TP} of Burnett (1998), above the FO of *Uniplanarius trifidus* in the same bed, and includes the inoceramid bed described above. This zonal and chronostratigraphic age attribution is also supported by the presence of *Ceratolithoides aculeus*, *C.* cf. *kamptneri*, *Eiffellithus eximius* and *Reinhardtites levis*.

PALAEOENVIRONMENTAL ANALYSIS

The overall composition of nannofossil and dinocyst assemblages, as well as palynofacies data are combined for palaeoenvironmental interpretations and settings (Tyson 1993, 1995). Numerous studies performed on Cretaceous dinoflagellate cyst assemblages have illustrated their utility to interpret the depositional environments in terms of water depth, depositional energy, sea surface temperature trend and productivity, by using the P/G ratio and the presence of environmentally sensitive dinocyst groups (e.g., Bujak 1984; Marshall and Batten 1988; Leereveld 1995; Pearce *et al.* 2003, 2009; Niechwedowicz *et al.* 2021).

Nannofossil palaeoenvironmental indicators

Nannofossil assemblages are dominated by *Watznaueria* spp. (1–3 specimens per FOV in better preserved samples) and more common *Calculites* spp., *Cribrosphaerella* spp., *Lucianorhabdu*s spp., *Micula* spp., *Prediscosphaera* spp., *Retecapsa crenulata* and *Zeugrhabdotus* spp. The predominance of *Watznaueria barnesae* (a warm-water species) and the rarity of typical low-latitude nannofossils such as *Uniplanarius* spp., *Ceratolithoides* spp., *Marthasterites* spp., and the occasional presence of cooler-water taxa like *Kamptnerius* spp. indicates a peri-Tethyan influence (Burnett 1998; Thibault *et al.* 2016; Švábenická *et al.* 2022). The stable presence of preferably shallow-marine holococcoliths such as *Lucianorhabdu*s spp. and *Calculites* spp. attests the link to more shallow, neritic shelf areas, although reworking and basin-ward transport into a more pelagic realm by turbidites may also be considered.

Dinocyst palaeoenvironmental proxies

Dinocyst assemblages from all productive samples in the Petrich section are dominated by representatives of the genera *Pterodinium* spp., *Spiniferites* spp., *Achomosphaera* spp. and *Cannosphaeropsis* spp., and to a lesser extent, by *Palaeohystrichophora infusorioides* spp. (Text-fig. 6). The species diversity is moderate, with 30 documented dinocyst species.

Marshall and Batten (1988) were among the first to notice that the dinocyst association can be directly related to the litho- and palynofacies. They recognized that the *Spiniferites*-dominated association, which generally occurs in chalks and marlstones that accumulated in an open marine environment, suggests the presence of well-oxygenated conditions in a stratified water column.

The frequent occurrence of *Spiniferites* spp., *Pterodinium* spp. and *P. infusorioides* in the European Upper Cretaceous successions allowed Pearce *et al*. (2003, 2009) and Prince *et al*. (2008) to identify two distinct types of assemblages based on diversity and assemblage composition. The first one was termed the '*Spiniferites–Palaeohystrichophora* (S-P) Assemblage' characterized by high diversities and abundances of gonyaulacoid (*Spiniferites*, *Achomosphaera*, *Pterodinium*) and peridinioid (especially *P. infusorioides*) cysts in the Cenomanian/Turonian boundary interval in the Anglo-Paris Basin, plus *Chatangiella*, *Isabelidinium*, *Trithyrodinium* in the North Sea. This assemblage contrasts to the low diversity '*Circulodinium–Heterosphaeridium* (C-H) Assemblages' that are typically dominated by gonyaulacoid cysts (*Circulodinium*, *Heterosphaeridium*). The authors analyzed these different types of dino-

cyst assemblages and estimated them as a marker of water depth, surface water nutrient levels and temperature trend. The S-P Assemblage was considered to be indicative for more basinal areas with unstable hydrodynamic conditions and higher, but variable, nutrient levels.

Following these studies, the encountered Petrich dinocyst association could be attributed in general to the S-P assemblages. It is characterized by high diversity and abundance of gonyaulacoid (*Pterodinium*, *Spiniferites*, *Achomosphaera*, *Cannosphaeropsis*) cysts (Text-fig. 6). The encountered low P/G ratio values in all samples, together with the presence, although subordinate, of high-productivity indicators like *P. infusorioides* indicates low nutrient levels and the development of a comparatively oligotrophic water mass within a distal neritic to open marine depositional environment. The occurrence of typical open oceanic dinocysts like *Pterodinium* confirms such conclusions (Harland 1983; Leereveld 1995; Niechwedowicz *et al*. 2021).

Palynofacies analysis

Palynofacies data corroborate well to the palaeoenvironmental interpretation. All samples from the Chugovitsa Formation and its Voden Member appeared to be rich in organic matter (OM). The organic matter is represented mainly by opaque phytoclasts and abundant dinoflagellate cysts with subordinate translucent phytoclasts, spores and woody tissues in the upper part of the succession. The opaque to translucent OP/TR ratio is high in all samples and especially in the sampling interval from bed 19 to bed 23 (samples P-7 to P-11; Text-fig. 3), where the highest amount of opaque phytoclasts and marine plankton is recognized, probably indicating a transgressive phase within this stratigraphical interval. Generally, the OP/TR ratio increases basin-wards due to fractionation processes and the higher preservation potential of opaque particles (Tyson 1993). Such a ratio is characteristic for distal shelf to open marine deposits. Opaque phytoclasts are typically equidimensional, rarely lath and of medium size. According to Tyson (1995) and Radmacher *et al*. (2020), a large proportion of equidimensional, small and rounded opaque phytoclasts points to the presence of a distal depositional environment that is located farther away from the continental source area. In the upper Campanian, corresponding to the interval from bed 25 to bed 37, a slight change occurs in the palynofacies composition (Text-fig. 9). The OP/TR ratio shows still high values, but opaque phytoclasts and dinocysts decrease slightly and large translucent structured phytoclasts as woody tissues and cuticles appear in the palynofacies. The continental input (influxes of structured translucent phytoclasts and spores) increases upwards in this interval, most probably indicating an increase in terrigenous influences during the late Campanian.

The distribution of palynofacies components is illustrated in the ternary AOM–Phytoclast –Palynomorph plot of Tyson (1993) and in the Microplankton–Spore–Pollen ternary plot (after Fedorova 1977; Duringer and Doubinger 1985; Text-fig. 9). Based on the phytoclast, palynomorph and AOM percentages, the samples plot mainly into field V reflecting the distal oxic shelf. Palaeoenvironmental interpretations are further analyzed by plotting on the Microplankton–Spore–Pollen diagram of Fedorova (1977) and Duringer and Doubinger (1985). The apparent predominance of the Microplankton group, mainly represented by dinoflagellate cysts, shows that all samples point to the offshore field. According to these data we can conclude that the inferred depositional environments in these plots suggests deposition within an oxic distal shelf to open marine low-energy environment. These data are in accordance to the palaeoenvironmental interpretations based on the dinocyst assemblages.

CONCLUSIONS

The Petrich section of the Central Srednogorie Zone (Bulgaria) records a continuous epiclastic, pelagic and turbiditic Upper Cretaceous sedimentation, spanning the middle Coniacian to the Campanian–Maastrichtian boundary. The section yielded high-resolution multistratigraphic data obtained from calcareous nannofossils, dinocysts and inoceramids, particularly in the Campanian. Nannofossils allowed to recognize the following standard nannofossil zones/subzones (zonation of Burnett 1998, with emendments by Thibault *et al.* 2016): 1) UC10–UC11ab (middle to upper Coniacian); 2) UC11c–UC12–UC13 (uppermost Coniacian to Santonian; 3) UC14a (lowermost Campanian), 4) UC14b^{TP}–UC15c^{TP} (lower Campanian to lower upper Campanian); 5) UC15d^{TP}–UC15e^{TP} (upper Campanian); 6) UC16a^{TP} of Thibault *et al*. (2016) (upper upper Campanian); and 7) UC16b^{TP} (lowermost Maastrichtian according to the emended zonation of Thibault *et al*. 2016).

The base of the Campanian is defined by the FO of *Broinsonia parca parca* (*Aspidolithus parcus par-*

cus of other authors) together with a special morphotype of *Calculites obscurus* in bed 11 of the Petrich section. Based on these data we can conclude that the Mirkovo Formation (CORB *sensu* Wang *et al*. 2011) has a Santonian to lower Campanian stratigraphic range.

The dinocyst record of the Petrich section indicates the *Areoligera coronata* Zone with a stratigraphical range from the upper parts of the lower Campanian to the upper Campanian and thus, a direct calibration to the UC14b^{TP}–UC16a^{TP} nannofossil subzones. The zone is indicated by the presence of the index species and ranges of other taxa, such as *Cannosphaeropsis utinensis*, *Palaeohystrichophora infusorioides*, *Odontochitina porifera*, *Corradinisphaeridium horridum*, *Hystrichodinium pulchrum*, *Achomosphaera fenestra*, *Raetiaedinium truncigerum*, *Pervosphaeridium pseudhystrichodinium*, *Chatangiella ditissima* and *Chatangiella tripartita.*

The collected inoceramids from the lower part of the Chugovitsa Formation are correlated to the interval of nannofossil subzones UC15d^{TP} and UC15e^{TP} of the lower upper Campanian, corresponding to a middle Campanian in the North American three-fold subdivision. The inoceramid assemblage dates the interval as the '*Inoceramus*' *azerbaydjanensis*–'*Inoceramus*' *vorhelmensis* Zone.

Palynological results based on the encountered dinocyst assemblages suggest a low-energy depositional environment and low nutrient levels indicating relatively oligotrophic conditions within a distal neritic to open marine depositional environment during the Campanian. Palynofacies data corroborate well, pointing to the presence of an oxic distal depositional environment, located farther away from the continental source area.

Nannofossil assemblages show a mixture of low-latitude and mid-latitude nannofossils and a predominance of warm-water species, and are regarded as peri-Tethyan.

Acknowledgements

This research was financed by the Bilateral Bulgarian–Austrian collaboration project 'Late Cretaceous palaeoclimate events and stage boundaries correlations – evidence from Tethyan key sections of Bulgaria and Austria" (KP-06-Austria/9) and is a contribution to IGCP 661 and IGCP 710. We are grateful to Dr. P. Gedl for his help for the palynological processing of the samples. Special thanks are due to Prof. I. Walaszczyk and Dr. M. Niechwedowicz for their valuable suggestions on the manuscript.

REFERENCES

Aliev, M.M. 1952. New *Inoceramus* species from the Campanian Stage of the north-western part of the Minor Caucasus. *Doklady Akademii Nauk Azerbaydjanskoy SSR*, **8** (11), 601–603. [In Russian]

Antonescu, E., Foucher, J.-C., Odin, G.S., Schiøler, P., Siegl-Farkas, A. and Wilson, G.J. 2001. Chapter C2d. Dinoflagellate cysts in the Campanian–Maastrichtian succession of Tercis les Bains (Landes, France), a synthesis. In: Odin, G.S. (Ed.), The Campanian–Maastrichtian stage boundary characterisation at Tercis les Bains (France) and correlation with Europe and other continents. *Developments in Paleontology and Stratigraphy*, **19**, 3–881.

Below, R. 1981. Dinoflagellaten-Zysten aus dem oberen Hauterive bis unteren Cenoman Süd-West-Marokkos. *Palaeontographica B*, **176**, 1–145.

Birkelund, T., Hancock, J.M., Hart, M.B., Rawson, P.F., Remane, J., Robaszynski, F., Schmid, F. and Surlyk, F. 1984. Cretaceous stage boundaries – Proposals. *Bulletin of the Geological Society of Denmark*, **33**, 3–20.

Böhm, J. 1907. Über *Inoceramus Cripsi* Mant. *Zeitschrift der Deutschen Geologischen Gesellschaft*, **59**, 113–114.

Bramlette, M.N. and Martini, E. 1964. The great change in calcareous nannoplankton fossils between the Maestrichtian and Danian. *Micropaleontology*, **10** (2), 291–322.

Brinkhuist, H. 1994. Late Eocene to Early Oligocene dinoflagellate cysts from the Priabonia type-area (Northeast Italy): biostratigraphy and paleoenvironmental interpretation. *Palaeogeography*, *Palaeoclimatology*, *Palaeoecology*, **107**, 121–163.

Bujak, J.P. 1984. Cenozoic dinoflagellate cysts and acritarchs from the Bering Sea and northern North Pacific. D.S.D.P. leg 19. *Marine Micropalaeontology*, **30**, 180–212.

Bukry, D. 1969. Upper Cretaceous coccoliths from Texas and Europe. *University of Kansas Paleontological Contributions*, **51** (Protista 2), 1–79.

Burnett, J.A. 1998. Upper Cretaceous: In: Bown, P.R. (Ed.), Calcareous Nannofossil Biostratigraphy (British Micropaleontological Society Publications Series), 132–199. Chapman and Kluwer Academic Publisher; London.

Christensen, W.K. 1999. Upper Campanian and Lower Maastrichtian belemnites from the Mons Basin, Belgium. *Bulletin de l'Institut Royal des Sciences Naturelles de Belgique*, **69**, 97–131.

Clarke, L.J. and Jenkyns H.C. 1999. New isotope oxygen evidence for long-term Cretaceous climatic change in Southern Hemisphere. *Geology*, **27** (8), 699–702.

Cobban, W.A., Walaszczyk, I., Obradovich, J.D. and McKinney, K.C. 2006. A USGS Zonal Table for the Upper Cretaceous Middle Cenomanian–Maastrichtian of the Western Interior of the United States based on Ammonites, Inoceramids and Radiometric Ages. *U.S. Geological Survey Open-File Report*, **2006-1250**, 48 pp.

Cookson, I.C. 1956. Additional microplankton from Australian

Late Mesozoic and Tertiary sediments. *Australian Journal of Marine and Freshwater Research*, **7** (**1**), 183–191.

Coquand, H. 1857. Position des *Ostrea columba* et *biauriculata* dans le groupe de la craie inférieure. *Bulletin de la Société géologique de France*, Ser. **2** (14), 745–766.

Corradini, D. 1973. Non-calcareous microplankton from the Upper Cretaceous of the northern Apennines. *Bollettino della Società paleontologica Italiana*, **11**, 119–197.

Davey, R.J. and Williams, G.L. 1966. The genera *Hystrichosphaera* and *Achomosphaera*. In: Davey, R.J., Downie, C., Sarjeant, W.A.S. and Williams, G.L. (Eds), Studies on Mesozoic and Cainozoic dinoflagellate cysts. *British Museum (Natural History) Geology*, *Bulletin*, Supplement **3**, 28–52.

Deflandre, G. 1935. Considérations biologiques sur les microorganisms d'origine planctonique conservés dans les silex de la craie. *Bulletin biologique de la France et de la Belgique*, **69**, 213–244.

Deflandre, G. 1937. Microfossiles des silex crétacés. Deuxième partie. Flagellés incertae sedis. Hystrichosphaeridés. Sarcodinés. Organismes divers. *Annales de paléontologie*, **26**, 51–103.

Deflandre, G. 1959. Sur les nannofossiles calcaires et leur systématique. *Revue de Micropaléontologie*, **2**, 127–152.

Dochev, D., Pavlishina, P., Petkanska, I. and Vladimirova, E. 2018. Preliminary results about the Campanian/Maastrichtian boundary in Reselets Section (Western Fore-Balkan), based on inoceramid bivalves, ammonites and dinoflagellate cysts. *Review of the Bulgarian Geological Society*, **79** (3), 87–88.

Duringer, P. and Doubinger, J. 1985. La palynologie: un outil de caractérisation des faciès marins et continentaux à la limite Muschelkalk supérieur – Lettenkohle. *Sciences Géologiques*, *bulletins et mémoires*, **38** (1), 19–34.

Evitt, W.R. 1963. A discussion and proposals concerning fossil dinoflagellates, hystrichospheres, and acritarchs, I. *National Academy of Sciences, Washington, Proceedings*, **49**, 158–164.

Farhan, A. 1987. Evolutionary Trend of the Genus *Lithastrinus* to the Genus *Uniplanarius*. *Abhandlungen der Geologischen Bundesanstalt*, **39**, 57–65.

Fedorova, V.A. 1977. The significance of the combined use of microphytoplankton, spores and pollen for differentiation of multi-facies sediments. In: Samoilovich, S.R. and Timoshin, N.A. (Eds), Questions of Phytostratigraphy. *Trudy Neftyanoi nauchnoissledovatelskii geologo-razvedochnyi Institut (VNIGRI)*, **398**, 70–88. [In Russian]

Fensome, R.A., Williams, G.L. and MacRae, R.A. 2019. The Lentin and Williams index of fossil dinoflagellates, 2019 edition. *AASP Contribution Series*, **50**, 1173 pp.

Forchheimer, S. 1972. Scanning electron microscope studies of Cretaceous coccoliths from the Köpingsberg Borehole No. 1, SE Sweden. *Sveriges Geologiska Undersökning, Series C*, **668** (65), 1–141.

Frieling, J. and Sluijs A. 2018. Towards quantitative environmental reconstructions from ancient non-analogue microfossil assemblages: Ecological preferences of Paleocene–Eocene dinoflagellates. *Earth-Science Reviews*, **185**, 956–973.

Gale, A.S., Kennedy, W.J. and Walaszczyk, I. 2021. Correlation of the Santonian–early Campanian of Texas, USA with Anglo-Paris Basin (United Kingdom) and other regions. *Newsletters on Stratigraphy*, **54** (4), 433–460.

Gale, A.S., Montgomery, P., Kennedy, W.J., Hancock, J.M., Burnett, J.A. and McArthur, J.M. 1995. Definition and global correlation of the Santonian–Campanian boundary. *Terra Nova*, **7,** 611–622.

Gale, A.S., Mutterlose, J., Batenburg, S., Gradstein, F.M., Agterberg, F.P., Ogg, J.G. and Petrizzo, M.R. 2020. The Cretaceous Period. In: Gradstein, F.M., Ogg, J.G., Schmitz, M.D. and Ogg, G.M. (Eds), Geologic Time Scale 2020, 1023–1086. Elsevier; Amsterdam.

Gardin, S. 2001. A Tethyan reference record for the Campanian and Maastrichtian stages: the Bottacione section (Central Italy); review of the data and new calcareous nannofossils results. In: Odin, G.S. (Ed.), The Campanian–Maastrichtian stage boundary characterisation at Tercis les Bains (France) and correlation with Europe and other continents. *Developments in Paleontology and Stratigraphy*, **19**, 3–881.

Gartner, S. 1968. Coccoliths and related calcareous nannofossils from Upper Cretaceous deposits of Texas and Arkansas. *University of Kansas Paleontological Contributions, Articles*, **48** (Protista 1), 1–56.

Giers, R. 1964. Die Groβfauna der Mukronatekride (unteres Obercampan) im östlichen Münsterland. *Fortschritte Geologie Rheinland und Westfalen*, **7**, 213–294.

Grossouvre, A. de 1901. Recherches sur la Craie supérieure. Partie 1: stratigraphie générale. Mémoires pour servir á l'explication de la carte géologique détaillée de la France, 1013 pp. Imprimerie Nationale; Paris.

Grün, W. and Allemann, F. 1975. The Lower Cretaceous of Caravaca (Spain): Berriasian Calcareous Nannoplankton of the Miravetes Section (Subbetic Zone, Prov. of Murcia). *Eclogae Geologicae Helvetiae*, **68**, 147–211.

Hancock, J.M. and Gale, A.S. 1996. The Campanian stage. *Bulletin de l'Institut Royal des sciences naturelles de Belgique*, *Sciences de la Terre*, **66**, 103–109.

Hardenbol, J., Thierry, J., Farley, M.B., Jacquin, T., Graciansky, P.-Ch. and Vail, P.R. 1998. Mesozoic and Cenozoic Sequence chronostratigraphic framework of European Basins. *SEPM, Special Publications*, **60**, 2–13.

Harland, R. 1983. Distribution maps of recent dinoflagellate cysts in bottom sediments from the North Atlantic Ocean and adjacent seas. *Palaeontology*, **26**, 321–387.

Harris, A.J. and Tocher, B.A. 1997. Palaeoenvironmental analysis of Late Cretaceous dinoflagellate cyst assemblages using high-resolution sample correlation from the Western Interior Basin, USA. *Marine Micropaleontology*, **48**, 127–148.

Haq, B.U., Hardenbol, J. and Vail, P.R. 1987. Chronology of fluctuating sea levels since the Triassic. *Science*, **235**, 1156–1167.

Hattner, J.G., Wind, F.H. and Wise, S.W. 1980. The Santonian–Campanian boundary: comparison of nearshore-offshore calcareous nannofossil assemblages. *Cahiers de Micropaléontologie*, **3**, 9–26.

Hattner, J.G. and Wise, S.W. 1980. Upper Cretaceous calcareous nannofossil biostratigraphy of South Carolina. *South Carolina Geology*, **24**, 41–117.

Hay, W.W. and Floegel, S. 2012. New thoughts about the Cretaceous climate and oceans. *Earth Science Review*, **115**, 262–272.

Houben, A.J.P., Quaijtaal, W., Wade, B.S., Schouten, S. and Brinkhuis, H. 2019. Quantitative organic-walled dinoflagellate cyst stratigraphy across the Eocene–Oligocene Transition in the Gulf of Mexico: A record of climateand sea level change during the onse of Antarctic glaciation. *Newsletters on Stratigraphy*, **52** (2), 131–154.

Huber, B.T., Norris, R.D. and MacLeod, K.G. 2002. Deep-sea paleotemperature record of extreme warmth during the Cretaceous. *Geology*, **30**, 123–126.

Ivanov, Ž. 2017. Tectonics of Bulgaria, 331 pp. Sofia University Press; Sofia. [In Bulgarian with English abstract]

Jagt, J.W.M., Walaszczyk, I., Yazykova, E.A. and Zatoń, M. 2004. Linking southern Poland and northern Germany: Campanian cephalopods, inoceramid bivalves and echinoids. *Acta Geologica Polonica*, **54**, 573–586.

Jenkyns, H.C., Gale, A.S and Corfield, R.M. 1994. Carbon- and oxygen-isotope stratigraphy of the English Chalk and Italia Scaglia and its palaeoclimatic significance. *Geological Magazine*, **131**, 1–34.

Jolkičev, N. 1962. Inoceramen aus dem Maastricht Bulgariens. *Travaux sur la Géologie de Bulgarie*, *Série Paléontologie*, **4**, 133–169. [In Bulgarian with German abstract]

Jurkowska, A. 2016. Inoceramid stratigraphy and depositional architecture of the Campanian and Maastrichtian of the Miechów Synclinorium (Southern Poland). *Acta Geologica Polonica*, **66**, 59–84.

Kirsch, K.-H. 1991. Dinoflagellatenzysten aus der Oberkreide des Helvetikums und Nordultrahelvetikums von Oberbayern. *Münchner Geowissenschaftliche Abhandlungen*, *Reihe A*, *Geologie und Paläontologie*, **22**, 1–306.

Kennedy, W.J., Tunoğlu, C., Walaszczyk, I. and Ertekín, I.K. 2007. Ammonite and inoceramid bivalve faunas from the Davutlar Formation of the Deveknai-Kastamonu area, northern Turkey and their biostratigraphical significance. *Cretaceous Research*, **28**, 861–894.

Lamolda, M.A., Paul, C.R.C., Peryt, D. and Pons, J.M. 2014. The Global Boundary Stratotype and Section Point (GSSP) for the base of the Santonian Stage, "Cantera de Margas", Olazagutia, northern Spain. *Episodes*, **37** (1), 2–13.

Leereveld, H. 1995. Dinoflagellate cysts from the Lower Cretaceous Rio Argos succession (SE Spain). Doctoral Dissertation, Universiteit Utrecht, 175 pp. LPP Contribution series 2, LPP Foundation; Utrecht.

Lejeune-Carpentier, M. 1938. L'etude microscopique des silex (6ieme note). Areoligera: nouveau genre d'Hystrichosphaeridee. *Annales de la Société Géologique de Belgique*, **61**, 163–174.

Lentin, J.K. and Williams, G.L. 1975. Fossil dinoflagellates: index to genera and species. Supplement 1. *Canadian Journal of Botany*, **53**, 2147–2157.

Lentin, J.K. and Williams, G.L. 1976. A monograph of fossil peridinioid dinoflagellate cysts. *Bedford Institute of Oceanography*, *Report Series*, **BI-R-75–16**, 1–237.

Lentin, J.K. and Williams, G.L. 1989. Fossil dinoflagellates: index to genera and species, 1989 edition. *American Association of Stratigraphic Palynologists*, *Contributions Series*, **20**, 1–473.

Manivit, H., Perch-Nielsen, K., Prins, B. and Verbeek, J. W. 1977. Mid Cretaceous calcareous nannofossil biostratigraphy. *Proceedings of the Koninklijke Nederlandse Akademie van Wetenschappen B*, **80** (3), 169–181.

Mansour, A. and Wagreich, M. 2022. Earth system changes during the cooling greenhouse phase of the Late Cretaceous: Coniacian–Santonian OAE3 subevents and organic carbon-rich versus organic carbon-poor deposition. *Earth-Science Reviews*, **229**, 104022.

Marshall, K. and Batten, D.J. 1988. Dinoflagellate cyst associations in Cenomanian–Turonian "black shale" sequences of Northern Europe. *Review of Palaeobotany and Palynology*, **54**, 85–103.

Masure, E. 1985. Kystes de dinoflagellés. In: Neumann, M., Platel, J.P. (co-ord.), Andreieff, P., Bellier, J.-P., Damotte, R., Lambert, B., Masure, E. and Monciardini, C. (Eds), Le Campanien stratotypique: étude lithologique et micropaléontologique. *Géologie Méditerranéenne*, **10**, 41–57.

Masure, E. 1986. *Corradinisphaeridium*, nouveau genre de dinoflagellés du Sénonien d'Italie et de France. *Revue de micropaléontologie*, **29**, 109–119.

Miniati, F., Petrizzo, R.P., Falzoni, F. and Erba, E. 2020. Calcareous plankton biostratigraphy of the Santonian–Campanian boundary interval in the Bottaccione section (Umbria-Marche Basin, Central Italy). *Rivista Italiana di Paleontologia e Stratigrafia*, **126** (3), 771–789.

Moev, M and Antonov, M. 1978. Stratigraphy of the Upper Cretaceous in the eastern part of the Stargel-Tshelopech strip. *Annual of the University of Mining and Geology, Faculty of Geology and Geophisics*, **28** (2), 7–30. [In Bulgarian with English abstract]

Mohamed, O. and Wagreich, M. 2013. Organic-walled dinoflagellate cyst biostratigraphy of the Well Höflein 6 in the Cretaceous–Paleogene Rhenodanubian Flysch Zone (Vienna Basin, Austria). *Geologica Carpathica*, **64** (3), 209–230.

Niechwedowicz, M. and Walaszczyk, I. 2022. Dinoflagellate cysts of the Upper Campanian-basal Maastrichtian (Upper Cretaceous) of the Middle Vistula River section (central Poland): statigraphic successions correlation potential and taxonomy. *Newsletters on Stratigraphy*, **55** (1), 21–67.

Niechwedowicz, M., Walaszczyk, I. and Barski, M. 2021. Phytoplankton response to palaeoenvironmental changes across the Campanian–Maastrichtian (Upper Cretaceous)

boundary interval of the Middle Vistula River section, central Poland. *Palaeogeography*, *Palaeoclimatology*, *Palaeoecology*, **577**, 110558.

Odin, G.S. (Ed.) 2001. The Campanian–Maastrichtian stage boundary characterisation at Tercis les Bains (France) and correlation with Europe and other continents. *Developments in Paleontology and Stratigraphy*, **19**, 3–881.

Odin, G.S. and Lamaurelle, M.A. 2001. The global Campanian–Maastrichtian stage boundary at Tercis les Bains, Landes, SW France. *Episodes*, **24** (4), 229–238.

Ogg, J.G. and Hinnov, L.A. 2012. Cretaceous. In: Gradstein, F.M., Ogg, J.G., Schmitz, M.D. and Ogg, G.B. (Eds), The Geological Time Scale 2012. Volume II, 793–853. Elsevier B.V.

d'Orbigny, A. 1842. Paléontologie francaise. Terrains crétacés. 2. Gastropodes, 456 pp. Masson; Paris.

Pavlishina, P., Dochev, D., Metodiev, L. and Vladimirova, E. 2020. Inoceramid bivalves and dinoflagellate cysts integrated biostratigraphy of the topmost Campanian–Maastrichtian in part of Western Fore-Balkan Mountains northwest Bulgaria. *Geologica Balcanica*, **49** (3), 39–63.

Pearce, M.A., Jarvis, I., Swan, A., Murphy, A., Tocher, B. and Edmunds, M.W. 2003. Integrating palynological and geochemical data in a new approach in palynological studies: Upper Cretaceous of the Banterwick Barn borehole, Berkshire, UK. *Marine Micropalaeontology*, **47**, 271–306.

Pearce, M.A., Jarvis, J. and Tocher, B.A. 2009. The Cenomanian–Turonian boundary event and palaeoenvironmental change in epicontinental seas: new insights from the dinocyst and geochemical records. *Palaeogeography*, *Palaeoclimatology*, *Palaeoecology*, **280**, 207–234.

Perch-Nielsen, K. 1968. Der Feinbau und die Klassifikation der Coccolithen aus dem Maastrichtien von Danemark. *Biologiske Skrifter*, *Kongelige Danske Videnskabernes Selskab*, **16**, 1–96.

Perch-Nielsen, K. 1979. Calcareous nannofossils from the Cretaceous between the North Sea and the Mediterranean: In Wiedmann, J. (Ed.), Aspekte der Kreide Europas. *International Union of Geological Sciences Series A*, **6**, 223–272.

Petrizzo, M.R., Falzoni, F. and Premoli-Silva, I. 2011. Identification of the base of the lower-to-middle Campanian Globotruncana ventricosa Zone: Comments on reliability and global correlations. *Cretaceous Research*, **32** (3), 387–405.

Peyrot, D. 2011. Late Cretaceous (Late Cenomanian–Early Turonian) dinoflagellate cysts from the Castilian Platform, northern Spain. *Palynology*, **35** (2), 267–300.

Premoli Silva, I. and Sliter, W.V. 1999. Cretaceous paleoceanography: Evidence from planktonic foraminiferal evolution. In: Barrera, E. and Johnson, C.C. (Eds), The Evolution of Cretaceous Ocean – Climatic System. *Geological Society of America, Special Paper*, **332**, 301–328.

Prince, I.M., Jarvis, I., Pearce, M.A. and Tocher, B.A. 2008. Dinoflagellate cyst biostratigraphy of the Coniacian–Santonian (Upper Cretaceous): New data from the English Chalk. *Review of Palaeobotany and Palynology*, **150**, 59–96.

Püttmann, T. and Mutterlose, J. 2021. Paleoecology of Late Cretaceous coccolithophores: Insights from the shallow-marine record. *Paleoceanography and Paleoclimatology*, **36** (3), e2020PA004161.

Radmacher, W., Kobos, K., Tyszka, J., Jarzynka, A. and Arz, J.A. 2020. Palynological indicators of palaeoenvironmental perturbations in the Basque-Cantabrian Basin during the latest Cretaceous (Zumaia, northern Spain). *Marine and Petroleum Geology*, **112**, 104–107.

Radmacher, W., Perez-Rodríguez, I., Arz, J. and Pearce, M., 2014. Dinoflagellate biostratigraphy at the Campanian–Maastrichtian boundary in Zumaia, northen Spain. *Cretaceous Research*, **51**, 309–320.

Reinhardt, P. 1966. Zur Taxonomie und Biostratigraphie des fossilen Nannoplanktons aus dem Malm, der Kreide und dem Alttertiär Mitteleuropas. *Freiberger Forschungshefte*, **C196**, 5–109.

Robaszynski, F., Bless, M.J.M., Felder, P.J., Foucher, J.-C., Legoux, O., Manivit, H., Meessen, J.P.M.T. and van der Tuuk, L.A. 1985. The Campanian–Maastrichtian boundary in the chalky facies close to the type-Maastrichtian area. *Bulletin des Centres de Recherches et d'Exploration-Production d' Elf-Aquitaine*, **9**, 1–113.

Roemer, F.A. 1852. Die Kreidebildungen von Texas und ihre organischen Einschlüsse, 100 pp. Adolph Marcus; Bonn.

Roncaglia, L. 2002. Lower Maastrichtian dinoflagellates from the Viano Clay Formation at Viano, northern Apennines, Italy. *Cretaceous Research*, **23**, 65–76.

Roncaglia, L. and Corradini, D. 1997. Correlation of key dinoflagellate events with calcareous nannoplankton and planktonic foraminiferal zones in the Solignano Formation (Maastrichtian, Late Cretaceous), northern Apennines, Italy. *Review of Palaeobotany and Palynology*, **97**, 177–196.

Sarjeant, W.A.S. 1970. The genus *Spiniferites* Mantell, 1850 (Dinophyceae). *Grana*, **10**, 74–78.

Schiøler, P., Brinkhuis, H., Roncaglia, L. and Wilson, G.J. 1997. Dinoflagellate biostratigraphy and sequence stratigraphy of the type Maastrichtian (Upper Cretaceous), ENCI Quarry, The Netherlands. *Marine Micropaleontology*, **31**, 65–95.

Schiøler, P. and Wilson, G.J. 2001. Dinoflagellate biostratigraphy around the Campanian–Maastrichtian boundary at Tercis les Bains, southwest France. In: Odin, G.S. (Ed.), The Campanian–Maastrichtian boundary: characterisation and correlation from tercis-les-Bains (Landes, SW France) to Europe and other continents. *Developments in Palaeontology and Stratigraphy*, **19**, 222–234.

Schlotheim, B.F. 1813. Beiträge zur Naturgeschichte der Versteinerungen in geognostischer Hinsicht. *Leonhard's Taschenbuch für die gesummte Mineralogie mit Hinsieht auf die neuesten Entdeckungen*, **7**, 1–134.

Schlotheim, E.F. 1820. Die Petrefactenkunde auf ihrem jetzigen Standpunkte: durch die Beschreibung seiner Sammlung versteinerter und fossiler Überreste des Thier- und Pflanzenreichs der Vorwelt erläutert, 1, 437 pp. Becker'she Buchhandlungen; Gotha.

Sissingh, W. 1977. Biostratigraphy of Cretaceous calcareous nannoplankton. *Geologie en Mijnbouw*, **56**, 37–65.

Skupien, P. and Mohamed, O. 2008. Campanian to Maastrichtian palynofacies and dinoflagellate cysts of the Silesian Unit, Outer Western Carpathians, Czech Republic. *Bulletin of Geosciences*, **83** (2), 207–224.

Slimani, H. 2001. Les Kystes de dinoflagelles du Campanien au Daniendans la region de Maastricht (Belgique, Pays-Bas) et de Turnhout (Belgique): biozonation et correlation avec d'autres regions en Europe occidentale. *Geologica et Palaeontologica*, **35**, 161–201.

Slimani, H., Louwye, S., Dusar, M. and Lagrou, D. 2011. Connecting the Chalk Group of the Campine Basin to the dinoflagellate cyst biostratigraphy of the Campanian to Danian in borehole Meer (northern Belgium). *Netherlands Journal of Geosciences-Geologie en Mijnbouw*, **90** (2/3), 129–164.

Slimani, H., M'Hamdi, A., Uchman, A., Gasiński, M.A., Guédé, K.É. and Mahboub, I. 2021. Dinoflagellate cyst biostratigraphy of Upper Cretaceous turbiditic deposits from a part of the Bąkowiec section in the Skole Nappe (Outer Carpathians, southern Poland). *Cretaceous Research*, **123**, 104780.

Sluijs, A., Pross, J. and Brinkhuis, H. 2005. From greenhouse to icehouse; organic-walled dinoflagellate cysts as paleoenvironmental indicators in the Paleogene. *Earth-Science Reviews*, **68**, 281–315.

Stover, L.E. and Evitt, W.R. 1978. Analyses of pre-Pleistocene organic-walled dinoflagellates. *Stanford University Publications, Geological Sciences*, **15**, 1–300.

Stover, L.E., Brinkhuis, H., Damassa, S.P., de Verteuil, L., Helby, R.J., Monteil, E., Partridge, A.D, Powell, A.J., Riding, J.B., Smelror, M. and Williams, G.L. 1996. Chapter 19. Mesozoic–Tertiary dinoflagellates, acritarchs and prasinophytes. In: Jansonius, J. and McGregor, D.C. (Eds), Palynology: principles and applications, vol. 2, 641–750. AASP Foundation.

Stradner, H. 1962. Über neue und wenig bekannte Nannofossilien aus Kreide und Alttertiär. *Verhandlungen der Geologischen Bundesanstalt*, **2**, 363–377.

Stradner, H. 1963. New contributions to Mesozoic stratigraphy by means of nannofossils. *Proceedings of the Sixth World Petroleum Congress. Section 1*, **4**, 167–183.

Švábenická, L., Wagreich, M. and Egger, H. 2002. Upper Cretaceous calcareous nannofossil assemblages at a transect from the northern Tethys to the temperate realm in Central Europe. In: Michalík, J. (Ed.), Tethyan/Boreal Cretaceous correlation. Mediterranean and Boreal Cretaceous palaeobiogeographic areas in Central and Eastern Europe, 187–212. VEDA Publishing House of the Slovak Academy of Sciences; Bratislava.

Thibault, N., Harlou, R., Schovsbo, N.H., Stemmerik, L. and Surlyk, F. 2016. Late Cretaceous (late Campanian–Maastrichtian) sea-surfaces temperature record of the Boreal Chalk Sea. *Climate of the Past*, **12**, 429–438.

Tsankov, V. 1981. Les fossilies de Bulgarie. V. Crétacé supérieur. Grandes foraminiféres, Anthozoaries, Gastéropodes, Bivalvia, 233 pp. Academie Bulgare des Sciences; Sofia. [In Bulgarian with French abstract]

Tyson, R. 1993. Palynofacies analysis. In: Jenkins, D.G. (Ed.), Applied Micropaleontology, 153–191. Kluwer Academic Publishers; Dordrecht, the Netherlands.

Tyson, R. 1995. Sedimentary organic matter. Organic facies and palynofacies, 615 pp. Chapman and Hall; London.

Vangelov, D., Gerdjikov, I., Dochev, D., Dotseva, Z., Velev, S., Dinev, Y., Tryanova, D. and Dancheva, J. 2019. Upper Cretaceous lithostratigraphy of the Panagyuriste strip (Central Bulgaria) – part of the Late Cretaceous Apuseni-Banat-Timok-Srednogorie magmatic belt. *Geologica Balcanica*, **48** (3), 11–33.

Vekshina, V.N. 1959. Coccolithophoridae of the Maastrichtian deposits of the West Siberian lowlands. *Trudyi Instituta Geologii i Geofiziki*, *Sibiriskoe Otlodelenie*, *Akademiya Nauk SSSR*, **2**, 56–81.

Vozzhennikova, T.F. 1967. Fossil peridinioides from Jurassic, Cretaceous and Paleogene deposits in USSR, 347 pp. Izdatelstvo Nauka; Moscow. [In Russian]

Wagreich, M. 2012. "OAE 3" – regional Atlantic organic carbon burial during the Coniacian–Santonian. *Climate of the Past*, **8**, 1447–1455.

Walaszczyk, I. 1992. Turonian trough Santonian deposits of the Central Polish Uplands; their facies development, inoceramid paleontology and stratigraphy. *Acta Geologica Polonica*, **42**, 1–122.

Walaszczyk, I. 1997. Biostratigraphie und Inoceramen des oberen Unter-Campan und unteren Ober-Campan Norddeutschlands. *Geologie und Paläontologie in Westfalen*, **49**, 1–117.

Walaszczyk, I. 2004. Inoceramids and inoceramid biostratigraphy of the Upper Campanian to basal Maastrichtian of the Middle Vistula River Section, central Poland. *Acta Geologica Polonica*, **54**, 95–168.

Walaszczyk, I., Cobban, W.A. and Harries, P.J. 2001. Inoceramids and inoceramid biostratigraphy of the Campanian and Maastrichtian of the United States Western Interior basin. *Revue Paléobiologie, Genève*, **20** (1), 117–234.

Walaszczyk, I., Cobban, W.A. and Odin, G.S. 2002. The inoceramid succession across Campanian–Maastrichtian boundary. *Bulletin of the Geological Society of Denmark*, **49**, 53–60.

Walaszczyk I., Cobban W.A., Wood, C.J. and Kin, A. 2008. The "*Inoceramus*" *azerbaydjanensis* fauna (Bivalvia) and its value for chronostratigraphic calibration of the European Campanian (Upper Cretaceous). *Bulletin de l'Institut Royal des sciences naturelles de Belgique*, *Sciences de la Terre*, **78**, 229–238.

Walaszczyk, I. and Dhondt, A.V. 2005. Santonian–Campanian (Upper Cretaceous) inoceramids from the Houthalen mineshaft, NE Belgium. *Bulletin de l'Institut Royal des sciences naturelles de Belgique, Sciences de la Terre*, **75**, 167–181.

Walaszczyk, I., Kennedy, W.J., Dembicz, K., Gale, A.S., Praszkier, T., Rasoamiaramana, A. and Randrianaly, H. 2014. Ammonite and inoceramid biostratigraphy and biogeogra-

phy of the Cenomanian through basal Middle Campanian (Upper Cretaceous) of the Morondava Basin, western Madagascar. *Journal of African Earth Sciences*, **89**, 79–132.

Walaszczyk, I., Odin, G.S. and Dhondt, A.V. 2002. Inoceramids from the Upper Campanian and Lower Maastrichtian of the Tercis section (SW France), the Global Stratotype Section and Point for the Campanian–Maastrichtian boundary and correlation potential. *Acta Geologica Polonica*, **52**, 269–305.

Wang, C., Hu, X., Huang, Y., Wagreich, M., Scott, R. and Hay, W. 2011. Cretaceous oceanic red beds as possible consequence of oceanic anoxic events. *Sedimentary Geology*, **235** (1–2), 27–37.

Wang, Z. and Young, M. 2013. Atlas of modern dinoflagellate cyst distribution based on 2405 data points. *Review of Palaeobotany and Palynology*, **191**, 1–197.

Wetzel, O. 1933. Die in organischer Substanz erhaltenen Mikrofossilien des baltischen Kreide-Feuersteins mit einem sediment-petrographischen und stratigraphischen Anhang. *Palaeontographica A*, **78**, 1–110.

Williams, G., Brinkhuis, H., Pearce, M., Fensome, R. and Weegink, W. 2004. Southern ocean and global dinoflagellate cyst events compared: Index events for the late Cretaceous–Neogene. *Proceedings of the Ocean Drilling Program, Scientific Results*, **189**, 1–98.

Wilpshaar, M. and Leereveld, H. 1994. Palaeoenvironmental change in the Early Cretaceous Vocontian Basin (SE France) reflected by dinoflagellate cysts. *Review of Palaeobotany and Palynology*, **84**, 121–128.

Wind, F.H. and Wise, S.W. 1983. Correlation of upper Campanian–lower Maestrichtian calcareous nannofossil assemblages in drill and piston cores from the Falkland Plateau, southwest Atlantic Ocean. *Initial Reports of the Deep Sea Drilling Project*, **71**, 551–563.

Wolfgring, E., Wagreich, M., Dinarès-Turel, J., Gier, S., Boehm, K., Sames, B., Spötl, Ch. and Popp, F. 2018. The Santonian–Campanian Boundary and the end of Long Cretaceous Normal Polarity Chron: Isotope and plankton stratigraphy of a pelagic reference section in the NW Tethys (Austria). *Newsletters on Stratigraphy*, **51** (4), 445–476.

Woods, H. 1910–1912. A Monograph of the Cretaceous Lamellibranchiata of England. *Monographs of Paleontological Society*, **2**, 261–340.

Yun, H. 1981. Dinoflagellaten aus der Oberkreide (Santon) von Westfalen. *Palaeontographica B*, **177**, 1–89.

Zonneveld, K.A.F., Marret, F., Versteegh, G.J.M, Bogus, K., Bonnet, S., Bouimetarhan, I., Crouch, E., de Vernal, A., Elshanawany, R., Edwards, L., Esper, O., Forke, S., Grøsfjeld, K., Henry, M., Holzwarth, U., Kielt, J.F., Kim, So-Y., Ladouceur, S., Ledu, D., Chen, L., Limoges, A., Londeix, L., Lu, S.-H., Mahmoud, M.S., Marino, G., Matsouka, K., Matthiessen, J., Mildenhal, D.C., Mudie, P., Neil, H.L., Pospelova, V., Qi, Y., Radi, T., Richerol, T., Rochon, A., Sangiorgi, F., Solignac, S., Turon, J.L., Verleye, T., Wang, Y. 2013. Atlas of modern dinoflagellate cyst distribution based on 2405 data points. *Review of Palaeobotany and Palynology*, **191**, 1–197.

Manuscript submitted: 21st March 2022
Revised version accepted: 5th July 2022

Appendix 1

List of calcareous nannofossil taxa encountered in the Petrich section, Bulgaria (according to Nannotax3: https://www.mikrotax.org/Nannotax3/)

Ahmuellerella octoradiata (Górka) Reinhardt, 1966
Arkhangelskiella cymbiformis Vekshina, 1959
Biscutum constans (Górka) Black in Black and Barnes, 1959
Biscutum cf. *melaniae* (Górka) Reinhardt, 1969
Braarudosphaera bigelowii (Gran and Braarud) Deflandre, 1947
Broinsonia enormis (Shumenko) Manivit, 1971
Broinsonia parca constricta Hattner, Wind and Wise, 1980
Broinsonia parca parca (Stradner) Bukry, 1969
Calculites obscurus (Deflandre) Prins and Sissingh in Sissingh, 1977
Calculites obscurus (Deflandre) Prins and Sissingh in Sissingh, 1977 – wide morphotype
Calculites ovalis (Stradner) Prins and Sissingh in Sissingh, 1977
Ceratolithoides aculeus (Stradner) Prins and Sissingh in Sissingh, 1977
Ceratolithoides kamptneri Bramlette and Martini, 1964
Chiastozygus litterarius (Górka) Manivit, 1971
Corollithion cf. *signum* Stradner, 1963
Cribrosphaerella circula (Risatti) Lees, 2007
Cribrosphaerella ehrenbergii (Arkhangelsky) Deflandre in Piveteau, 1952
Cylindralithus sp.
Eiffellithus eximius (Stover) Perch-Nielsen, 1968
Eiffellithus gorkae Reinhardt, 1965
Eiffellithus turriseiffelii (Deflandre in Deflandre and Fert) Reinhardt, 1965
Eprolithus floralis (Stradner) Stover, 1966
Gartnerago sp.
Helicolithus cf. *trabeculatus* (Górka) Verbeek, 1977
Kampnerius sp.
Lithastrinus grillii Stradner, 1962
Lithraphidites carniolensis Deflandre, 1963
Lithraphidites praequadratus Roth, 1978
Lucianorhabdus cayeuxii Deflandre, 1959
Lucianorhabdus cayeuxii Deflandre, 1959 – curved morphotype
Lucianorhabdus maleformis Reinhardt, 1966
Manivitella pemmatoidea (Deflandre in Manivit) Thierstein, 1971
Marthasterites inconspicuus Deflandre, 1959
Microrhabdulus decoratus Deflandre, 1959
Micula cf. *adumbrata* Burnett, 1997
Micula cubiformis Forchheimer, 1972
Micula staurophora (Gardet) Stradner, 1963
Micula cf. *swastica* Stradner and Steinmetz, 1984
Operculodinella sp.
Placozygus spiralis (Bramlette and Martini) Hoffmann, 1970
Prediscosphaera cretacea (Arkhangelsky) Gartner, 1968
Prediscosphaera grandis Perch-Nielsen, 1979
Quadrum cf. *gartneri* Prins and Perch-Nielsen in Manivit *et al*., 1977
Reinhardtites levis Prins and Sissingh in Sissingh, 1977
Retecapsa crenulata (Bramlette and Martini) Grün in Grün and Allemann, 1975
Rhagodiscus angustus (Stradner) Reinhardt, 1971
Rhagodiscus sp.
Rucinolithus sp.

Staurolithites sp.
Tranolithus minimus (Bukry) Perch-Nielsen, 1984
Tranolithus orionatus (Reinhardt) Reinhardt, 1966
Uniplanarius gothicus (Deflandre) Hattner and Wise in Wind and Wise, 1983
Uniplanarius sissinghii (Perch-Nielsen) Farhan, 1987
Uniplanarius trifidus (Stradner in Stradner and Papp) Hattner and Wise in Wind and Wise, 1983
Watznaueria barnesae (Black in Black and Barnes) Perch-Nielsen, 1968
Zeugrhabdotus diplogrammus (Deflandre in Deflandre and Fert) Burnett in Gale *et al*., 1996
Zeugrhabdotus embergeri (Noël) Perch-Nielsen, 1984
Zeugrhabdotus erectus (Deflandre in Deflandre and Fert) Reinhardt, 1965

Appendix 2

List of dinoflagellate cyst taxa encountered in the Petrich section, Bulgaria

Achomosphaera crassipellis (Deflandre and Cookson) Stover and Evitt, 1978
Achomosphaera fenestra Kirsch, 1991
Achomosphaera sagena Davey and Williams, 1966
Achomosphaera ramulifera (Deflandre) Evitt, 1963
Achomosphaera regiensis Corradini, 1973
Areoligera coronata (Wetzel) Lejeune-Carpentier, 1938
Cannosphaeropsis utinensis Wetzel, 1933
Chatangiella ditissima (McIntyre) Lentin and Williams, 1976
Chatangiella tripartita (Cookson and Eisenack) Lentin and Williams, 1976
Corradinisphaeridium horridum (Deflandre) Masure, 1986
Exochosphaeridium majus (Lejeune-Carpentier) Peyrot, 2011
Hystrichodinium pulchrum Deflandre, 1935
Hystrichosphaeridium duplum Lentin and Williams, 1989
Hystrichosphaeridium salpingophorum (Deflandre) Deflandre, 1937 emend. Davey and Williams, 1966
Hystrichosphaeridium tubiferum (Ehrenberg) Deflandre, 1937
Isabelidinium cooksoniae (Alberti) Lentin and Williams, 1977
Odontochitina porifera Cookson, 1956
Oligosphaeridium complex (White) Davey and Williams, 1966
Oligosphaeridium pulcherrimum (Deflandre and Cookson) Davey and Williams, 1966
Palaeohystrichophora infusorioides Deflandre, 1935
Pervosphaeridium monasteriense Yun, 1981
Pervosphaeridium pseudhystrichodinium (Deflandre) Yun, 1981
Pterodinium cingulatum (Wetzel) Below, 1981
Raetiaedinium truncigerum (Deflandre) Kirsch, 1991
Spiniferites membranaceus (Rossignol) Sarjeant, 1970
Spiniferites ramosus (Ehrenberg) Mantell, 1854
Spiniferites scabrosus (Clarke and Verdier) Lentin and Williams, 1975
Surculosphaeridium longifurcatum (Firtion) Davey, Downie, Sarjeant and Williams, 1966
Tanyosphaeridium regulare Davey and Williams, 1966